TH17 Panel 1 (mouse) Kits

IL-16, IL-17A, IL-17C, IL-17E/IL-25, IL-17F, IL-21, IL-22, IL-23, IL-31, MIP-3α

V-PLEX®

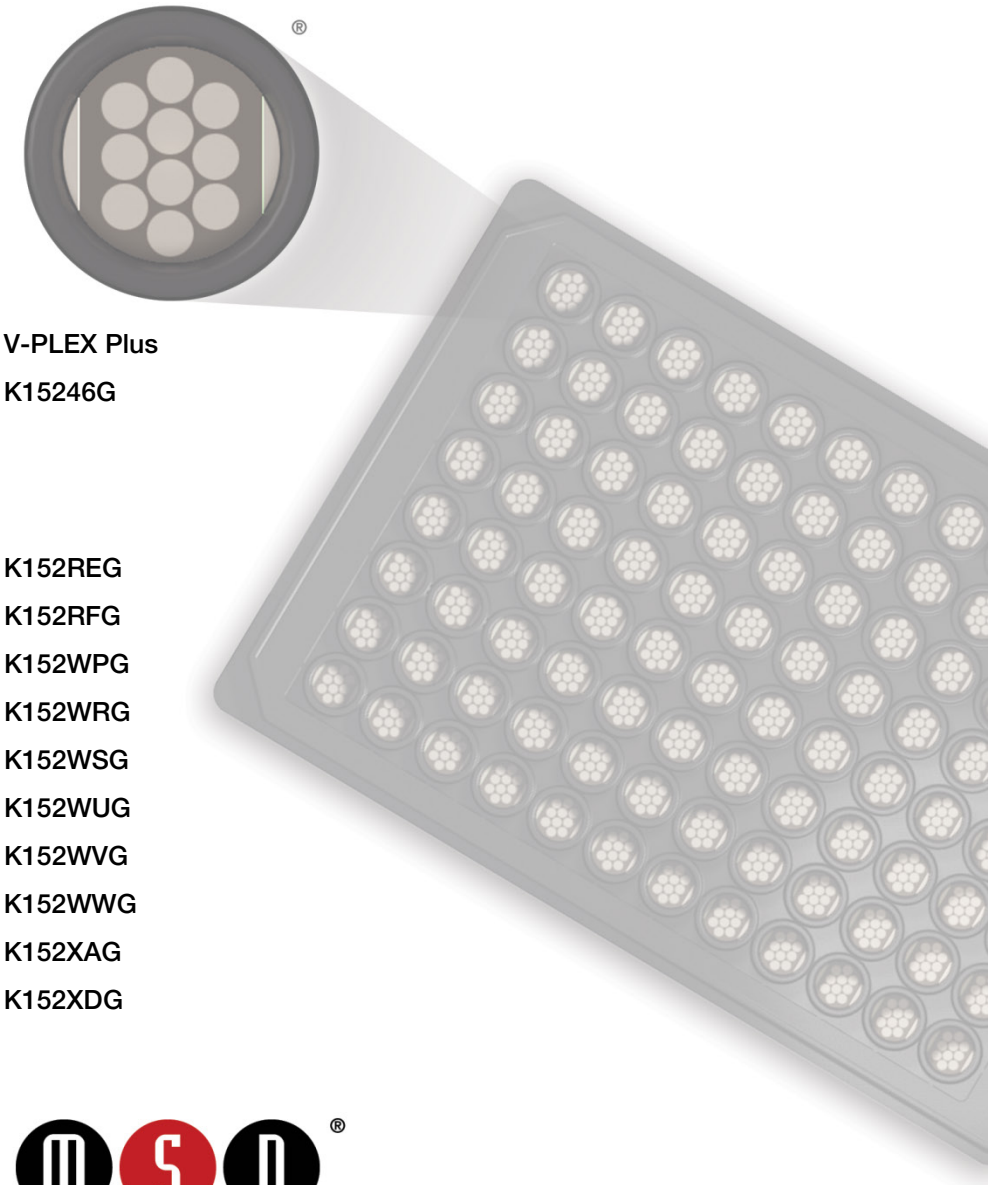

	V-PLEX®	V-PLEX Plus
TH17 Panel 1 (mouse)	K15246D	K15246G
Individual Assay Kits		
Mouse IL-16	K152RED	K152REG
Mouse IL-17A	K152RFD	K152RFG
Mouse IL-17C	K152WPD	K152WPG
Mouse IL-17E/IL-25	K152WRD	K152WRG
Mouse IL-17F	K152WSD	K152WSG
Mouse IL-21	K152WUD	K152WUG
Mouse IL-22	K152WVD	K152WVG
Mouse IL-23	K152WWD	K152WWG
Mouse IL-31	K152XAD	K152XAG
Mouse MIP-3α	K152XDD	K152XDG

MSD Cytokine Assays

TH17 Panel 1 (mouse) Kits

IL-16, IL-17A, IL-17C, IL-17E/IL-25, IL-17F, IL-21, IL-22, IL-23, IL-31, MIP-3α

For use with mouse cell culture supernatants, serum, plasma, and urine.

This package insert must be read in its entirety before using this product.

FOR RESEARCH USE ONLY.

NOT FOR USE IN DIAGNOSTIC PROCEDURES.

MESO SCALE DISCOVERY®
A division of Meso Scale Diagnostics, LLC.
1601 Research Blvd.
Rockville, MD 20850 USA
www.mesoscale.com

Table of Contents

Contact Information

MSD Customer Service

Phone: 1-240-314-2795
Fax: 1-301-990-2776
Email: CustomerService@mesoscale.com

MSD Scientific Support

Phone: 1-240-314-2798
Fax: 1-240-632-2219 attn: Scientific Support
Email: ScientificSupport@mesoscale.com

Introduction

MSD offers V-PLEX assays for customers who require unsurpassed performance and quality. V-PLEX products are developed under rigorous design control and are analytically validated according to fit-for-purpose principles in accordance with MSD's Quality Management System. They offer exceptional sensitivity, simple protocols, reproducible results, and lot-to-lot consistency. In addition to the analytical validation, robustness of the assay protocol is assessed during development along with the stability and robustness of the assay components and kits. V-PLEX assays are available in both single-assay and multiplex formats.

The V-PLEX assay menu is organized by panels. Grouping the assays into panels by species, analytical compatibility, clinical range, and expected use, ensures optimal and consistent performance from each assay while still providing the benefits and efficiencies of multiplexing. V-PLEX panels are provided in MSD's MULTI-SPOT® 96-well plate format. The composition of each panel and the location of each assay (i.e., its spot within the well) are maintained from lot to lot. Most Individual V-PLEX assays are provided on MSD's single-spot, 96-well plates. The remaining are provided on the multiplex panel plate.

The TH17 Panel 1 (mouse) measures ten cytokines that are important in TH17 pathways. TH17 cells are a critical part of the immune system and act as a bridge between the innate and adaptive immune systems. Improper regulation of their proinflammatory activities contributes to numerous pathogenic conditions such as rheumatoid arthritis, psoriasis, type 1 diabetes, multiple sclerosis, Crohn's disease, and asthma. As a result of their association with such a wide spectrum of disease, these biomarkers are the subjects of drug discovery projects, diagnostics development, and basic research. The biomarkers constituting the panel are described below.

Mouse interleukin-16 (IL-16), also known as Lymphocyte chemoattractant factor (LCF), predominantly exists as a non-covalently linked homotetramer consisting of individual 14 kDa subunits (130 amino acids each) under physiologic conditions. Some IL-16 may exist in the monomeric or dimeric form[1]. IL-16 is synthesized as a precursor molecule (pro-IL-16) of approximately 68 kDa (631 amino acids) lacking a signal peptide and is strongly expressed by majority of unstimulated blood CD4 & CD8 T cells[2]. After cell activation via the T cell receptor, precursor IL-16 is cleaved by caspase-3, which produces mature IL-16 (derived from the C-terminal 121 amino acids) and pro–IL-16 (N-terminal domain of the precursor molecule). Both the pro-IL-16 and mature forms have been found to be biologically active. The pro-IL-16 does not exhibit lymphocyte chemoattractant activity[2] but contains the nuclear localization sequence (NLS) and functions as a transcriptional repressor with regulatory effects on cell cycle progression[1]. Mature IL-16, which is the secreted 121-amino acid C-terminal peptide, then autoaggregates to form the bioactive multimers. Multimerization occurs intracellularly prior to secretion and is facilitated by the PDZ domains. During inflammatory responses, the predominant sources of IL-16 are peripheral blood mononuclear cells from spleen, thymus, and lymphoid tissue. Other hematopoietic cells including eosinophils, dendritic cells, mast cells, macrophages, monocytes, fibroblasts, neuronal cells, and bronchial epithelial cells can also secrete IL-16 under certain conditions[1]. Mature IL-16 is a chemotactic factor for CD4+ T cells, monocytes, dendritic cells and eosinophils and has been shown to upregulate IL-2Rα (CD25) on CD4 T cells[3]. Although the main receptor for IL-16 appears to be the CD4 molecule that is expressed on Th cells, monocytes and other phagocytes, functional activity of IL-16 independent of CD4 has been demonstrated[4]. The structural and functional similarity between murine and human IL-16 indicate that it is highly conserved between these species[5]. IL-16 secreted by the neuronal cell results in increased cell survival, proliferation and growth of the neurons. Although a physiologic role for neuronal IL-16 has not been clearly defined, it has been found to be upregulated in microglial cells in association with inflammatory brain lesions[1]. IL-16 signals through the CD4 associated p56lck/Protein kinase C pathway. The downstream signaling involves mobilizing intracellular Ca^{2+}, IP3, and PI3K activation[1,6].

IL-16 expression was found to be significantly increased in the inflamed colonic mucosa of inflammatory bowel disease (IBD) patients (ulcerative colitis and Crohn's disease) as compared to control individuals, and patients under steroid treatment. Local expression of IL-16 thus seems to play a significant role in the initiation and persistence of the inflammatory process in Crohn's disease[4,7]. It has been shown that in rheumatoid arthritis (RA) and Graves' disease (GD), serum IgG antibodies can stimulate synovial fibroblasts to produce increased levels of IL-16, RANTES and IL-6 through the insulin like growth factor receptor 1 (IGF-R1) pathway. The resulting infiltration of the T cells in the synovial tissue could promote inflammation in the affected tissue[8]. Using a murine model of pneumonia, a recent study demonstrated that MRSA (methicillin-resistant S. aureus) acutely induced CD4 T cells to produce IL-16 in the lung, resulting in potentially damaging inflammatory response to the infection. S. aureus directly activated TNFR1, as well as the Ca/calpain/caspase signaling cascade, to release of IL-16. It is thus postulated that in inflammatory conditions involving excessive TNF signaling, such as IBD, IL-16 contributes significantly to the pathology[9]. IL-16 has been identified in the airway epithelium and bronchoalveolar lavage in human and murine allergic airway inflammation and IL-16 is proposed to be a natural modulator of Th2 cell-mediated airway inflammation[10].

In multiple myeloma patients, where IL-16 functions as a growth factor for CD4 and/or CD9-expressing malignant plasma cells in the bone marrow, the elevated serum levels of IL-16 correlated with increased disease severity[1]. In cutaneous T cell lymphomas (CTCL), mutation in the IL-16 gene prevented the nuclear translocation of pro-IL-16 resulting in a hyperproliferative state and resulted in elevated levels of mature IL-16 in serum[1]. It has been demonstrated that the recombinant C-terminal 130 amino acid of human and simian IL-16 were capable of suppressing HIV-1 replication in CD8+ depleted PBMCs. It was later shown that the secretion of IL-16 (and not the intracellular form) is required for HIV inhibition[1,11].

Mouse interleukin-17A (IL-17A) is the signature cytokine of the Th17 cell subset. The IL-17 family of cytokines is emerging as key players in the host defense against microbial organisms and in the pathogenesis of inflammatory diseases. The family consists of six members IL-17A, IL-17B, IL-17C, IL-17D, IL-17E/IL-25, and IL-17F. These molecules share 16–50% homology to IL-17A with IL-17F being the most homologous to IL-17A[12,13]. IL-17A exists as a disulfide-linked biologically active homodimer (IL-17AA) or forms a biologically active heterodimer with IL-17F (IL-17AF)[13]. IL-17A, IL-17F and IL-17A/F all signal through the same heterodimeric receptor complex, IL-17RA and IL-17RC. However, IL-17A and IL-17F have distinct biological effects. The functional differences between IL-17A and IL-17F may be explained on the basis of strength of signaling triggered by the two cytokines. IL-17A responses are 10–30 fold stronger in terms of downstream gene activation than those of IL-17F, with IL-17AF heterodimers acting at an intermediate level. Both IL-17A and IL-17F signal through the engagement of Act1/TRAF6 and activation of the MAPK/ERK/NF-κB pathways[14]. Although the IL-17RA and IL-17RC subunits are expressed as a heterodimeric complex, these subunits have reciprocal expression patterns, suggestive of tissue-dependent activities. Unlike IL-17RA that is expressed at high levels in haematopoietic tissues, IL-17RC expression is low in haematopoietic tissues and high in non-immune cells of the prostate, liver, kidney, thyroid and joints[14]. IL-17A & IL-17F are co-expressed when naïve CD4 T cells are cultured under Th17 polarizing conditions (IL-6 or IL-21 plus TGF-β)[15]. Although in mice TGF-β and IL-6 are required for lineage commitment of Th17 cells, subsequent exposure to IL-23 and IL-1 is necessary for full effector differentiation and function of Th17 cells[16]. In addition to Th17 cells, a wide variety of T cell subsets, neutrophils, monocytes, lymphoid tissue inducer (LTi)-like cells, and intestinal epithelial cells produce IL-17A and IL-17F. IL-17A is also produced by the Paneth cells in the intestine[13,15].

The protective role of IL-17A in host defense has been demonstrated in various infection models. Mice deficient in IL-17 receptor (IL-17R) expression are susceptible to infection by various pathogens[17]. In a mouse model of allergic airway inflammation it was demonstrated that IL-23 and Th17 cells not only induce Th17-cell-mediated neutrophilic airway inflammation but also up-regulate Th2-cell-mediated eosinophilic airway inflammation[18]. Expression of IL-17A, IL-17C, and IL-17F is increased in psoriatic lesions. Successful treatment resulted in restoration of several downstream signaling genes to near normal levels[19,20]. In individuals with rheumatoid arthritis, plasma levels of IL-17A, IL-17A/F, and IL-17F were all significantly increased when compared with controls[73]. IL-17A is an important therapeutic target in autoimmunity. Treatment with a neutralizing anti-IL-17 antibody in murine model of

collagen-induced arthritis (CIA) significantly reduced the severity of the disease[21]. Treatment with secukinumab (human monoclonal anti-IL-17A antibody) resulted in rapid and sustained resolution of symptom in individuals with psoriasis, rheumatoid arthritis, psoriatic arthritis, and ankylosing spondylitis[22]. In a mouse model of metastatic breast cancer, treatment with anti-IL-17A neutralizing antibody resulted in significant reduction in metastasis[23]. Th17 cells are a subset of the Tumor infiltrating lymphocytes (TIL) population. The intensity of TIL infiltration in tumors often correlates with the stage of the disease. Within the tumor microenvironment, the infiltrating Th17 cells are frequently located at the proximity to the tumor mass. High IL-17 levels in blood or presence of IL-17-secreting cells in tumor microenvironment is reported to have a negative impact on prognosis of several cancers. IL-17/IL-17R axis is thus emerging as an immunotherapeutic target for cancer[24].

Mouse interleukin-17C (IL-17C) is an autocrine cytokine, and a member of the IL-17 cytokine family[19]. Although the functions are less understood, increasing evidence supports the role of IL-17C in Th17 differentiation and mucosal defense. It has only 26% homology with the IL-17A[13]. IL-17C is expressed in CD4+ T cells, DCs, and macrophages at inflammatory sites, but not in most normal tissues[13]. It is also induced in epithelial cells by bacterial challenge and inflammatory stimuli[19]. Binding of IL-17C to the IL-17RA/IL-17RE receptor complex results in the recruitment of the adapter molecule, Act1, at the cytoplasmic tail and subsequent activation of NFκB pathway. This leads to the expression of target genes that play a role in the innate host defense mechanism. The IL-17RE/IL-17RA complex is expressed on keratinocytes, epithelial, and Th17 cells[25,26]. IL-17C signaling through its receptor IL-17RE has been shown to be involved in the regulation of differentiation and potentiation of the Th17 cellular response. The IL17C/IL17RE signaling also plays a role in pathogenesis of autoimmune diseases as demonstrated in the EAE model. The regulation of Th17 differentiation and inflammation was mediated through signaling components Act1 and induction of IkBζ[26]. IL-17C, like IL-17A and IL-17F, has been demonstrated to act on keratinocytes to induce human β-defensin 2 and granulocyte colony–stimulating factor[19]. Both IL-17C and IL-17B induce TNF-α and IL-1β expression from a monocytic cell line and cause neutrophil infiltration[13].

IL-17C has been demonstrated to act on keratinocytes to induce proinflammatory cytokines, chemokines, and AMPs (anti-microbial peptides). IL-17C-/- mice had significantly decreased inflammation and epidermal thickening in the imiquimod psoriasis-like model. Expression of IL-17A, IL-17C, and IL-17F is increased in psoriatic lesions. Successful treatment resulted in restoration of several downstream signaling genes to near normal levels[19,20]. In a mouse model of lupus, local production of IL-17 cytokines (IL-17A and IL-17C) in the kidneys induced inflammation by recruitment of neutrophils and monocytes. IL-17C was postulated to exacerbate the inflammatory process by enhancing IL-17 production from infiltrating CD4+ T cells and responsible for the development of fatal lupus pathology[27]. The IL-17C-IL-17RE signaling pathway may thus be a promising target in the treatment of chronic autoimmune diseases[26]. In a metastatic lung cancer model, it was shown that tumor proliferation and growth as well as the number of tumor-associated neutrophils were significantly decreased in IL-17C-/- mice. The study also demonstrated that human lung cancer samples stained positive for IL-17C. In non-small cell lung cancer patients with lymph node metastasis, IL-17C was reported to be a negative prognostic factor[28].

Mouse interleukin-17E/25 (IL-17E/IL-25) is a member of the IL-17 family of cytokines and bears least (16%) homology to the principle cytokine of the family, IL-17A. It does not share common functions of the IL-17 cytokine family but promotes Th2 type immune responses[13,15]. The IL-17E receptor is a heterodimer consisting of IL-17RA and IL-17RB[14,15]. Although IL-17E binds only IL-17RB, but not IL-17RA, both chains are essential for signal transduction[13]. Like other IL-17 family receptors, signaling takes place through the recruitment of Act1/TRAF6 and activation of NF-κB. IL-17E is produced by Th2 cells, cecal patch CD4+ and CD8+ T cells, mast cells, and eosinophils. Additionally, in rodents, alveolar macrophages, endothelial, and epithelial cells can also produce IL-17E. In addition to promoting Th2 cell immune responses by activating Th2 cells and inducing Th2 cell cytokines (IL-4, IL-5, and IL-13) in auxiliary cells, IL-17E also induces IgE production and eosinophilia, contributing to the host defense against intestinal parasites[13]. IL-17E also promotes Th9 cells activation and can induce IL-5- and IL-13-mediated eosinophilia independently of T cells.

In chronic spontaneous urticaria (CSU) patients, marked elevations in the numbers of IL-17E+, IL-33+, and TSLP+ cells were observed in the dermis. This rise in Th2-initiating cytokines was reflected in the increases in cells expressing Th2 cytokine (IL-4 and IL-5) in skin lesions of these patients. Th2-initiating cytokines play a role in mast cell activation, inflammation, and vascular leakage in CSU[94]. Although IL-17E and IL-17A are members of the same cytokine family, they play opposing roles in the pathogenesis of organ specific autoimmunity. In NOD mice, the autoimmune diabetes model, islet-reactive Th17 cells have been demonstrated to promote pancreatic inflammation. In this model, anti IL-17A had no effect but IL-25 therapy restored normoglycemia in newly diabetic animals and significantly delayed recurrent autoimmunity after islet transplantation[95]. In the model for relapse-remitting autoimmune encephalomyelitis (EAE), IL-25 treatment completely suppressed disease[96]. The function of IL-25 in asthma has been well established. In a murine model of persistent allergic airway disease, allergen exposure upregulated both pulmonary expression of IL-25 and induced the accumulation of IL-25 driven IL-4/IL-13 producing steroid resistant pathogenic IL-17RB+ Type 2 granulocyte population in the lung. IL17RB-/- allergic mice exhibited a dramatic reduction in peribronchial and perivascular inflammation, eosinophilic infiltrates, and mucus production. In humans, IL-4/IL-13 producing granulocytes are also identified in the peripheral blood of asthmatics[97,98]. In breast cancer cells, it was shown that IL-25 treatment induced apoptosis in IL-25R expressing cells without causing toxicity to the nonmalignant cells. In addition it was demonstrated that high levels of IL-25R correlated with poor prognosis, suggesting that the IL-25/IL-25R signaling pathway could be a target for treating breast cancer[99]. Analysis of the signaling pathways indicated that both IL-17E and IL-17A promoted proliferation and survival of breast cancer cells via induction of tumorogenic low molecular weight forms of cyclin E and the phosphorylation of c-RAF, ERK1/2, and p70 S6 kinase[100].

Mouse interleukin-17F (IL-17F)is a cytokine belonging to the IL-17 family and has the highest sequence homology (50%) with IL-17A, the best characterized member of the IL-17 family[13]. IL-17F exists as a disulfide-linked biologically active homodimer (IL-17FF) or forms a biologically active heterodimer with IL-17A (IL-17AF)[13]. IL-17A, IL-17F and IL-17A/F all signal through the same heterodimeric receptor complex, IL-17RA and IL-17RC. However, IL-17A and IL-17F have distinct biological effects. The functional differences between IL-17A and IL-17F may be explained on the basis of strength of signaling triggered by the two cytokines. IL-17F responses are 10–30 fold weaker in terms of downstream gene activation than those of IL-17A, with IL-17A–IL-17F heterodimers acting at an intermediate level[14].

Activation of naïve CD4 T cells under Th17 polarizing conditions (IL-6 or IL-21 plus TGF-β) leads to strong expression of IL-17F where it is co-expressed with IL-17A in ~ 60% the Th17 cells[15]. In addition to Th17 cells, a wide variety of T cell subsets, neutrophils, monocytes, lymphoid tissue inducer (LTi)-like cells and intestinal epithelial cells also produce IL-17A and IL-17F[13,15]. Like IL-17A, IL-17F is also considered to be a proinflammatory cytokine since it induces many proinflammatory cytokines, chemokines, and neutrophil recruitment[13,15]. IL-17F acts synergistically with IL-22 to induce synthesis of antimicrobial peptides in keratinocytes[20,29]. Both IL-17A and IL-17F are major players in host defense against bacterial and fungal pathogens[30]. IL-17F target tissues include epithelial cells, fibroblasts, keratinocytes, synoviocytes and endothelial cells[13]. Although the IL-17RA and IL-17RC subunits are expressed as a heterodimeric complex, these subunits have reciprocal expression patterns, suggestive of tissue-dependent activities. Unlike IL-17RA that is expressed at high levels in haematopoietic tissues, IL-17RC expression is low in haematopoietic tissues and high in non-immune cells of the prostate, liver, kidney, thyroid and joints[14]. Both IL-17A and IL-17F signal through the engagement of Act1/TRAF6 and activation of the MAPK/ERK/NF-κB pathways[14].

IL-17F is expressed in the airway of asthmatics and its expression level is correlated with disease severity. The role of IL-17F in allergic airway inflammation is demonstrated as its overexpression in the airway of mice is associated with airway neutrophilia, the induction of cytokines, an increase in airway hyperreactivity, and mucus hypersecretion. Human asthma and chronic obstructive pulmonary disease, both associated with IL-17A, have been linked to mutations in the IL-17F gene[30]. Single nucleotide polymorphisms (SNPs) in the IL-17 gene have been shown to be correlated with susceptibility to cancer. Recent studies have reported that IL-17F can also induce the expression of various chemokines, cytokines, and adhesion molecules involved in inflammation-related cancer. A recent study showed that IL-17F -/- mice exhibited increased colonic tumors and tumor area

possibly by inhibiting tumor angiogenesis, indicating a protective role for IL-17F in colon tumorigenesis[31]. The rs763780 variant in the IL-17F gene can lead to a substitution that inhibits the function of wild-type IL-17F, leading to increased risk of several malignant tumors including gastric cancer, colorectal cancer, and breast cancer[32]. In the gut, IL-17 can exacerbate or protect from intestinal inflammation. IL-17A, IL-17F, and Th17 cells are upregulated in the intestinal mucosa of Crohn's disease and ulcerative colitis patients. In mice, IL-17F-/- animals were protected from dextran sodium sulfate induced autoimmune colon pathology[12]. Expression of IL-17A, IL-17C, and IL-17F is increased in psoriatic lesions. Successful treatment resulted in restoration of several downstream signaling genes to near normal levels[19,20]. In rheumatoid arthritis patients, plasma levels of IL-17A, IL-17A/F, and IL-17F were all significantly increased when compared with controls. However in synovial fluid, only IL-17F was found to be higher when compared with controls. In response to therapy with disease-modifying antirheumatic drugs (DMARDs), IL-17F (but not IL17A or A/F) selectively decreased in clinical responders[33].

Mouse interleukin-21 (IL-21) is a type I cytokine produced by activated CD4+ T cell subsets including Th17 cells, and follicular Th cells and natural killer T (NKT) cells[34,35]. Although the expression of IL-21R is restricted to lymphoid tissues and peripheral blood mononuclear cells, other tissues such as epithelium, synovium, or transformed cells can acquire expression of both components of IL-21R heterodimer[36]. It has pleiotropic effects on several cell types including, but not limited to, CD4+/CD8+ T cells, B cells, macrophages, monocytes, and dendritic cells (DCs). IL-21 plays a major role in B-cell differentiation, especially in the transition of B cells to plasma cells[37]. IL-21 also plays a role in the proliferation and maturation of natural killer (NK) cells[38]. IL-21 enhances cytotoxic activity and IFN-γ production by activated murine NK cells. IL-21 also limits NK cell responses by limiting their duration of activation and preventing IL-15-induced expansion of resting NK cells. By promoting antigen-specific T cell activation and simultaneously limiting NK cell responses, IL-21 regulates the transition from innate to adaptive immunity[39]. The functional receptor for IL-21 is a heterodimeric complex composed of the IL-21 receptor (IL-21R) and the common cytokine receptor γ chain (γc)[34]. The critical role of IL-21 in host defense is well demonstrated in individuals with primary immunodeficiency caused by IL-21 or IL-21R mutations[34,40]. Similar to other γc cytokines, IL-21 signals through the Janus kinase and Signal Transducer and Activator of Transcription (JAK-STAT), phosphoinositide 3-kinase (PI3K), and mitogen-activated protein kinase (MAPK) pathways. IL-21 induces strong and sustained activation of STAT3, which is critical for its effects on B-cell and T-cell differentiation[34].

The role for IL-21 in the pathogenesis of cancer has been extensively examined. IL-21 expands antitumor capabilities by enhancing cytotoxicity of NK cells and acting synergistically with IL-15, and expands antigen-specific CD8+ T-cells and their effector function. This has been demonstrated in humans as well as mouse models[34,41,42]. Multiple studies using animal models have established that IL-21 signaling promotes the pathogenesis of autoimmune diseases and overproduction of IL-21 in inflammatory bowel diseases (IBD), psoriasis, rheumatoid arthritis (RA), type I diabetes (T1DM) and systemic lupus erythematosus (SLE) has been demonstrated[34,43]. Using a mouse model of transient focal brain ischemia, it was demonstrated that IL-21 is highly up-regulated in the injured mouse brain after cerebral ischemia and brain-infiltrating CD4+ T-cells were the predominant source of IL-21[44], making it a candidate marker for brain injury. Recently IL-21 has also been shown to be a major player in transplantation. It was observed that morbidity and mortality of GVHD was significantly reduced after bone marrow transplant with splenocytes from IL-21R-/- mice compared with those from wild type mice[45]. In the late phase of alloimmune response, elevated IL-21 expands effector T cells and inhibits the differentiation /function of the Treg population. This ultimately results in suppression of tolerance induction essential in transplantation. Blockade of the IL-21/IL-21R pathway could be a precondition for tolerogenic protocols in transplantation[46]. IL-21 alone or in combination with other agents for treating metastatic cancers has been tested in clinical trials, and blocking antibodies to IL-21R are now being evaluated in clinical trials for the treatment of autoimmune diseases. IL-21 is thus a "double-edged sword" as modulating the IL-21/IL21R axis may lead to either the induction or suppression of immune responses[47].

Mouse interleukin-22 (IL-22), first described as IL-10-related T cell inducible factor[48], is part of the IL-10 superfamily notable for its opposing pro-inflammatory or anti-inflammatory actions, which are dependent on the context of its expression. In addition to the subsets of Th1, Th17 and the Th22 cells[49], IL-22 is produced by several types of immune cells including $\gamma\delta$ T cells, innate lymphoid cells, NKT cells, NK cells, macrophages, neutrophils and dendritic cells[50,51]. IL-22 binds heterodimer IL-22R that is made up of IL-22R1 and IL-10R2[52]. Although IL-10R2 is constitutively expressed in cells throughout the body, IL-22RA1 is expressed almost

exclusively in epithelial tissues thus indicating a role in the innate immunity of the epithelium[51]. The signaling pathway of IL-22R involves the Janus associated kinase 1 (Jak1), tyrosine kinase 2 (Tyk2) and the signal transducer activator of transcription 3 (STAT3). Additional pathways involved in IL-22 signaling include Mitogen Activation Protein Kinase (MAPK), Akt, and p38. IL-22 Binding Protein (IL-22BP or IL-22RA2) is a soluble secreted receptor that is structurally similar to the membrane bound IL-22RA1. It inhibits the binding of IL-22 to its receptor complex and blocks IL-22 signaling. IL-22BP levels decrease with significant increases in IL-22[51].

IL-22 concentration in synovial fluid and serum is higher in rheumatoid / psoriatic arthritis patients than in osteoarthritic or normal patients[53,54]. This is thought to be the result of the induction of RANKL and increased osteoclast production leading to joint inflammation[,54]. In contrast, IL-22 plays a protective and anti-fibrotic role in alcohol induced liver injury[55]. IL-22 is required for the onset of allergic asthma and its role in allergic airway inflammation is complex. Blocking expression of IL-22 early (sensitization phase) in allergic airway inflammation models reduces eosinophil recruitment, Th2 cytokine (IL-13 and IL-33), airway hyperreactivity, and mucus production. However, blocking during challenge phase exacerbates the disease and recombinant IL-22 given during the challenge phase protects mice from lung inflammation[56].

Mouse interleukin-23 (IL-23) is a heterodimeric cytokine that is structurally and functionally related to IL-12 family. Both share the 40 kDa (p40) subunit of IL-12. The active IL-23 molecule is composed of the p40 subunit and the 19 kDa (p19) subunit linked via disulfide linkage[16]. IL-23 is produced by activated monocytes, macrophages and dendritic cells in response to certain bacterial and viral components (including LPS, peptidoglycan, CpG DNA and poly I:C) through activation of toll-like receptors (TLRs)[57]. The IL-23 receptor complex is a heterodimer made up of IL-23R (unique for IL-23, binds to p19) and IL-12Rβ1 (shared with IL-12, binds to p40) subunits. The signaling pathway of IL-23R involves the Janus associated kinase 2 (Jak2), tyrosine kinase 2 (Tyk2) and several members of the signal transducer activator of transcription (STAT) family[58]. Although in mice TGF-β and IL-6 are required for lineage commitment of Th17 cells, subsequent exposure to IL-23 and IL-1 is necessary for full effector differentiation and function of Th17 cells[16].

The IL-23/IL-17 pathway is important to the mucosal host defense against extracellular pathogens[59]. IL-23 & IL-12 play a key role in sustaining inflammatory responses that link innate and adaptive immunity[60]. The role of the IL-23/IL-17 axis in autoimmunity has been demonstrated in humans and animal models of autoimmune diseases such as multiple sclerosis, rheumatoid arthritis, inflammatory bowel disease, and diabetes[57]. Thus, the IL-23/Th17 axis is considered as an important therapeutic target in autoimmune diseases, and bio therapeutics blocking IL-23 or IL-17 are currently being developed[61]. Over-expression of IL-23 (not IL-12) by macrophages and DCs in human and mouse tumors plays a role in promoting angiogenesis, tumor growth and reducing tumor infiltration of CD8+ T cells[57].

Mouse interleukin-31 (IL-31) is a four-helix bundle cytokine that belongs to the gp130/IL-6 cytokine family. All the members of this family share the common chain of glycoprotein 130 (gp130) in their multi-unit receptor complexes (except for IL-31 that uses gp130-like receptor[62,63]. Although IL-31 is predominantly secreted by the Th2 cells from the peripheral blood and skin-homing CLA+CD45RO+ T cells, it is also produced by Th22 cells, CD8 T cells, mast cells, monocytes/macrophages, eosinophils, germinal center(GC) B cells, immature/mature dendritic cells, keratinocytes and a variety of other tissues (skin, lung, small intestine, and the nervous system)[62,63]. Its production is induced by IL-4 and IL-33. IL-31 signals through a heterodimeric receptor composed of IL-31 receptor A (IL-31RA) and shared oncostatin M receptor (OSMAR). Signaling by IL-31 activates the JAK-STAT, the RAS/ERK, and the PI3K/AKT pathways[63,64]. IL-31RA is widely expressed (trachea, skeletal muscle, thymus, peripheral blood lymphocytes, placenta, bone marrow, thyroid, testis, brain, keratinocytes, eosinophils, mast cells, and dendritic cells)[63].

The role of IL-31 pruritus is well-defined[63,65,66]. IL-31 transgenic mice overexpressing IL-31 exhibit a skin phenotype closely resembling atopic dermatitis in human subjects[66]. IL-31 has been shown to effectively induced the secretion of chemokines, proinflammatory cytokines and matrix metalloproteinases from human colonic subepithelial myofibroblasts that play a role in inflammation / wound healing in the intestine. Th2-derived IL-31 and Th17-derived IL-17A are postulated to thus cooperate in the

pathophysiology of IBD[67]. IL-31 has recently been implicated in bronchial inflammation. In human bronchial epithelial cells, IL-31 alone or in combination with Th2 cytokines (IL-4 and IL-13) and eosinophils elevated the expression of EGF, VEGF, and MCP-1, and activates MAPK protein, in a time and dose dependent manner. Activation of the MAPK signaling pathway and production of inflammatory mediators, suggest that IL-31 may be a new target for development of therapeutic agent for treatment in allergic asthma[68].

Recently it has been shown that in cutaneous T cell lymphoma patients, tumor cells produce IL-31, and the serum levels of the cytokine correlate with pruritus intensity[63]. IL-31 selectively enhanced the proliferation of primary follicular lymphoma (FL) cells through IL-31R signaling but did not do so in normal germinal center derived B cells in spite of IL-31R expression. An autocrine role of IL-31/IL-31RA complex in tumor progression in follicular lymphoma (FL) has thus been suggested[69].

Mouse macrophage inflammatory protein 3 (MIP-3α/LARC/CCL20) is a C-C chemokine and the CCL20-CCR6 axis is responsible for the chemoattraction of immature dendritic cells (DC), effector/memory T-cells, and B-cells and plays a critical role at skin and mucosal surfaces under normal and pathological conditions[70]. Initially identified in the liver as liver activation regulated chemokine (LARC). MIP-3α is expressed in thymus, skin and intestinal tissues[71,72] In the CNS, it is constitutively expressed in the epithelial cells of choroid plexus and in murine autoimmune encephalomyelitis it is expressed by astrocytes[73–75]. In mouse and human, alternative splicing results in two transcripts: encoding LARC and its variant LARCvar, corresponding to with and without an N-terminal alanine in the mature protein, respectively[71]. Both types of transcripts appeared to be expressed in various mouse tissues. To date, MIP-3α is the only known ligand for the G protein-coupled receptor CCR6 receptor[76]. In addition to its expression on CD4 T-cells and B-cells, CCR6 is also expressed in intestine, colon, appendix, thymus, skin and liver. In peripheral blood, CCR6 is expressed on lymphoid but not on myeloid cells. CCR6 is highly expressed on immature dendritic cells (DC) but not on terminally differentiated DC[77,78].

MIP-3α is implicated in a broad spectrum of disorders, including colorectal cancer and tumor metastasis[79,80], rheumatoid arthritis[81], psoriasis[82], obesity[83,84], wound healing[85], colitis[86], and dry eye disease[87]. The CCL20-CCR6 axis has also been shown to be an important aspect of the innate immune defense against pneumococcal meningitis where it controls leukocyte recruitment and leukocyte-mediated bacterial killing in an IL17-independent manner[88]. Disrupting the MIP-3α and CCR6 interaction may prove to be a therapeutic strategy in some cases, as CCR6 deletion resulted in reduction in mouse atherosclerotic lesions[89] and enhanced immunity to RSV with reduced lung pathology[90].

Principle of the Assay

MSD cytokine assays provide a rapid and convenient method for measuring the levels of protein targets within a single, small-volume sample. The assays in the TH17 Panel 1 (mouse) are sandwich immunoassays. MSD provides a plate pre-coated with capture antibodies on independent and well-defined spots, as shown in the layout below. Multiplex assays and the individual MIP-3α, IL-17C, IL-31, IL-21, IL-17F, IL-16, and IL-17E/IL-25 assays are provided on 10-spot MULTI-SPOT plates (Figure 1); the individual IL-22, IL-23, and IL-17A assays are provided on Small Spot plates (Figure 2). The user adds the sample and a solution containing detection antibodies conjugated with electrochemiluminescent labels (MSD SULFO-TAG™) over the course of one or more incubation periods. Analytes in the sample bind to capture antibodies immobilized on the working electrode surface; recruitment of the detection antibodies by the bound analytes completes the sandwich. The user adds an MSD buffer that creates the appropriate chemical environment for electrochemiluminescence and loads the plate into an MSD instrument where a voltage applied to the plate electrodes causes the captured labels to emit light. The instrument measures the intensity of emitted light (which is proportional to the amount of analyte present in the sample) and provides a quantitative measure of each analyte in the sample. V-PLEX assay kits have been validated according to the principles outlined in "Fit-for-Purpose Method Development and Validation for Successful Biomarker Measurement" by J. W. Lee, et al.[91]

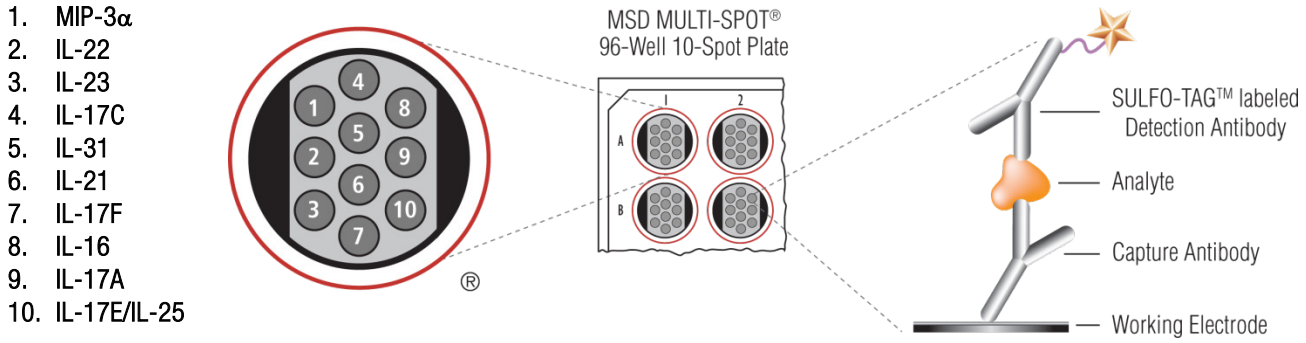

Figure 1. Multiplex plate spot diagram showing placement of analyte capture antibodies. The numbering convention for the different spots is maintained in the software visualization tools, on the plate packaging, and in the data files.

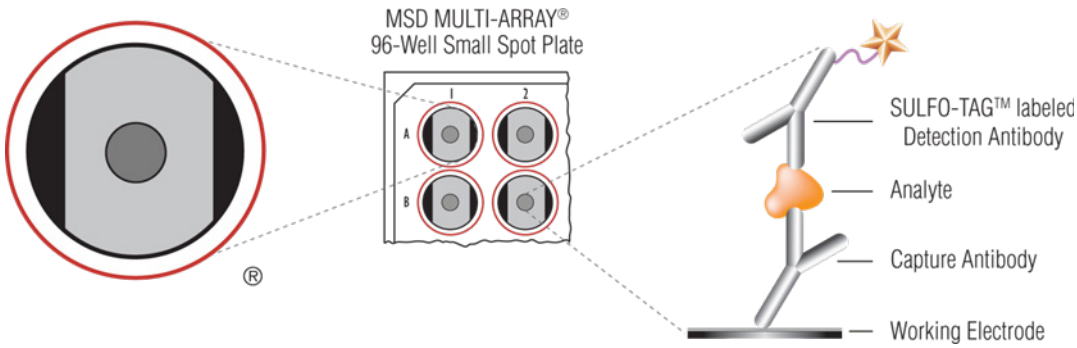

Figure 2. Small Spot plate diagram showing placement of analyte capture antibodies.

Kit Components

TH17 Panel 1 (mouse) assays are available as a multiplex kit, as individual assay kits, or as custom V-PLEX kits with subsets of assays selected from the full panel. V-PLEX Plus kits include additional items (controls, wash buffer, and plate seals). See below for details.

Reagents Supplied With All Kits

Table 1. Reagents that are supplied with V-PLEX and V-PLEX Plus Kits

Reagent	Storage	Catalog #	Size	Quantity Supplied			Description
				1-Plate Kit	5-Plate Kit	25-Plate Kit	
TH17 Panel 1 (mouse) Calibrator Blend	2–8 °C	C0246-2	1 vial	1 vial	5 vials	25 vials	Ten recombinant mouse proteins in diluent, buffered and lyophilized. Individual analyte concentration is provided in the lot-specific certificate of analysis (COA).
Diluent 41	≤-10 °C	R50AH-1	10 mL	1 bottle			Diluent for samples and calibrator; contains protein, blockers, and preservatives.
		R50AH-2	50 mL		1 bottle	5 bottles	
Diluent 45	≤-10 °C	R50AI-1	5 mL	1 bottle			Diluent for detection antibody; contains protein, blockers, and preservatives.
		R50AI-2	25 mL		1 bottle	5 bottles	
Read Buffer T (4X)	RT	R92TC-3	50 mL	1 bottle	1 bottle	5 bottles	Buffer to catalyze the electro-chemiluminescence reaction.

V-PLEX Plus Kits: Additional Components

Table 2. Additional components that are supplied with V-PLEX Plus Kits

Reagents	Storage	Catalog #	Size	Quantity Supplied			Description
				1-Plate Kit	5-Plate Kit	25-Plate Kit	
TH17 Panel 1 (mouse) Control 1*	2–8 °C	C4246-1	1 vial	1 vial	5 vials	25 vials	Multi-analyte controls in a non-mouse matrix, buffered, lyophilized, and spiked with recombinant mouse analytes. The control concentrations are provided in the lot-specific COA.
TH17 Panel 1 (mouse) Control 2*	2–8 °C	C4246-1	1 vial	1 vial	5 vials	25 vials	
TH17 Panel 1 (mouse) Control 3*	2–8 °C	C4246-1	1 vial	1 vial	5 vials	25 vials	
Wash Buffer (20X)	RT	R61AA-1	100 mL	1 bottle	1 bottle	5 bottles	20-fold concentrated phosphate buffered solution with surfactant.
Plate Seals	-	-	-	3	15	75	Adhesive seals for sealing plates during incubations.

*Provided as components in the TH17 Panel 1 (mouse) Control Pack (catalog # C4246-1)

Kit-Specific Components

Table 3. Components that are supplied with specific kits

Plates	Storage	Part #	Size	Quantity Supplied 1-Plate Kit	5-Plate Kit	25-Plate Kit	Description
TH17 Panel 1 (mouse) SECTOR® Plate	2–8 °C	N05246A-1	10-spot	1	5	25	96-well plate, foil sealed, with desiccant.
Mouse IL-17A SECTOR Plate	2–8 °C	L452RFA-1	Small Spot	1	5	25	
Mouse IL-22 SECTOR Plate	2–8 °C	L452WVA-1	Small Spot	1	5	25	
Mouse IL-23 SECTOR Plate	2–8 °C	L452WWA-1	Small Spot	1	5	25	

Table 4. Kits are supplied with individual detection antibodies for each assay ordered

SULFO-TAG Detection Antibody	Storage	Catalog #	Size	Quantity Supplied 1-Plate Kit	5-Plate Kit	25-Plate Kit	Description
Anti-ms IL-16 Antibody (50X)	2–8 °C	D22RE-2	75 µL	1			SULFO-TAG conjugated antibody
		D22RE-3	375 µL		1	5	
Anti-ms IL-17A Antibody (50X)	2–8 °C	D22RF-2	75 µL	1			SULFO-TAG conjugated antibody
		D22RF-3	375 µL		1	5	
Anti-ms IL-17C Antibody (50X)	2–8 °C	D22WP-2	75 µL	1			SULFO-TAG conjugated antibody
		D22WP-3	375 µL		1	5	
Anti-ms IL-17E/IL-25 Antibody (50X)	2–8 °C	D22WR-2	75 µL	1			SULFO-TAG conjugated antibody
		D22WR-3	375 µL		1	5	
Anti-ms IL-17F Antibody (50X)	2–8 °C	D22WS-2	75 µL	1			SULFO-TAG conjugated antibody
		D22WS-3	375 µL		1	5	
Anti-ms IL-21 Antibody (50X)	2–8 °C	D22WU-2	75 µL	1			SULFO-TAG conjugated antibody
		D22WU-3	375 µL		1	5	
Anti-ms IL-22 Antibody (50X)	2–8 °C	D22WV-2	75 µL	1			SULFO-TAG conjugated antibody
		D22WV-3	375 µL		1	5	
Anti-ms IL-23 Antibody (50X)	2–8 °C	D22RJ-2	75 µL	1			SULFO-TAG conjugated antibody
		D22RJ-3	375 µL		1	5	
Anti-ms IL-31 Antibody (50X)	2–8 °C	D22XA-2	75 µL	1			SULFO-TAG conjugated antibody
		D22XA-3	375 µL		1	5	
Anti-ms MIP-3α Antibody (50X)	2–8 °C	D22XD-2	75 µL	1			SULFO-TAG conjugated antibody
		D22XD-3	375 µL		1	5	

Additional Materials and Equipment

- ❑ Appropriately sized tubes for reagent preparation
- ❑ Polypropylene microcentrifuge tubes for preparing dilutions
- ❑ Liquid handling equipment for desired throughput, capable of dispensing 10 to 150 µL/well into a 96-well microtiter plate
- ❑ Plate washing equipment: automated plate washer or multichannel pipette
- ❑ Microtiter plate shaker (rotary) capable of shaking at 500–1,000 rpm
- ❑ Phosphate-buffered saline (PBS) plus 0.05% Tween-20 for plate washing or MSD Wash Buffer catalog # R61AA-1 (included in V-PLEX Plus kit)
- ❑ Adhesive plate seals (3 per plate included in V-PLEX Plus kits)
- ❑ Deionized water
- ❑ Vortex mixer

Optional Materials and Equipment

- ❑ TH17 Panel 1 (mouse) Control Pack, available for separate purchase from MSD, catalog # C4246-1 (included in V-PLEX Plus kit)
- ❑ Centrifuge (for sample preparation)
- ❑ De-crimping tool for opening calibrator and control vials

Safety

Use safe laboratory practices and wear gloves, safety glasses, and lab coats when handling kit components. Handle and dispose of all hazardous samples properly in accordance with local, state, and federal guidelines.

Additional product-specific safety information is available in the safety data sheet (SDS), which can be obtained from MSD Customer Service or at www.mesoscale.com.

Best Practices

- Do not mix or substitute reagents from different sources or different kit lots. Lot information is provided in the lot-specific COA.
- Assay incubation steps should be performed between 20-26 °C to achieve the most consistent signals between runs.
- Bring frozen diluent to room temperature in a 24 °C water bath. Thaw other reagents on wet ice and use as directed without delay.
- Prepare calibrators, samples, and controls in polypropylene microcentrifuge tubes; use a fresh pipette tip for each dilution; vortex after each dilution before proceeding.
- Avoid prolonged exposure of detection antibody (stock or diluted) to light. During the antibody incubation step, plates do not need to be shielded from light except for direct sunlight.
- Avoid bubbles in wells at all pipetting steps. Bubbles may lead to variable results; bubbles introduced when adding Read Buffer T may interfere with signal detection.
- Do not touch the pipette tip on the bottom of the wells when pipetting into the MSD plate.
- Use reverse pipetting when necessary to avoid introduction of bubbles. For empty wells, pipette to the bottom corner.
- Plate shaking should be vigorous, with a rotary motion between 500 and 1,000 rpm. Binding reactions may reach equilibrium sooner if you use shaking at the middle of this range (~700 rpm) or above.
- When using an automated plate washer, rotate the plate 180 degrees between wash steps to improve assay precision.
- Gently tap the plate on a paper towel to remove residual fluid after washing.
- Read buffer should be at room temperature when added to the plate.
- Keep time intervals consistent between adding read buffer and reading the plate to improve inter-plate precision. Unless otherwise directed, read plate as soon as practical after adding read buffer.
- No shaking is necessary after adding read buffer.
- If an incubation step needs to be extended, avoid letting the plate dry out by keeping sample or detection antibody solution in the plate.
- Remove the plate seals prior to reading the plate.
- If assay results are above the top of the calibration curve, dilute the samples and repeat the assay.
- When running a partial plate, seal the unused sectors (see sector map in instrument and software manuals) to avoid contaminating unused wells. Remove all seals before reading. Partially used plates may be sealed and stored up to 30 days at 2–8 °C in the original foil pouch with desiccant. You may adjust volumes proportionally when preparing reagents.

Reagent Preparation

Bring all reagents to room temperature.

Important: Upon first thaw, aliquot Diluent 41 and Diluent 45 into suitable volumes before refreezing.

Prepare Calibrator Dilutions

MSD supplies a multi-analyte lyophilized calibrator that yields the recommended highest calibrator concentration when reconstituted in 1,000 µL of Diluent 41. (For individual assays that do not saturate at the highest calibrator concentration, the calibration curve can be extended by creating a more concentrated highest calibrator. In this case, follow the steps below using 250 µL instead of 1,000 µL of Diluent 41 when reconstituting the lyophilized calibrator. This method is not recommended for the IL-21 assay.) Keep reconstituted calibrator and calibrator solutions on wet ice until use.

To prepare 7 calibrator solutions plus a zero calibrator for up to 4 replicates:

1) Prepare the highest calibrator (Calibrator 1) by adding 1,000 µL of Diluent 41 to the lyophilized calibrator vial. After reconstituting, invert at least 3 times (do not vortex). Let the reconstituted solution equilibrate at room temperature for **30-45 minutes** and then vortex briefly using short pulses.

   Note: It is critical that the reconstituted calibrator equilibrates at room temperature for 30-45 minutes prior to first use. Reconstituted calibrator is stable when stored at 2–8 °C up to 9 days. It may also be stored frozen at ≤-70 °C in suitable aliquots and subjected to up to 3 freeze–thaw cycles.

2) Prepare the next calibrator by transferring 100 µL of the highest calibrator to 300 µL of Diluent 41. Mix well by vortexing. Repeat 4-fold serial dilutions 5 additional times to generate 7 calibrators.

3) Use Diluent 41 as the zero calibrator.

Note: For the lot-specific concentration of each calibrator in the blend, refer to the COA supplied with the kit. You can also find a copy of the COA at www.mesoscale.com.

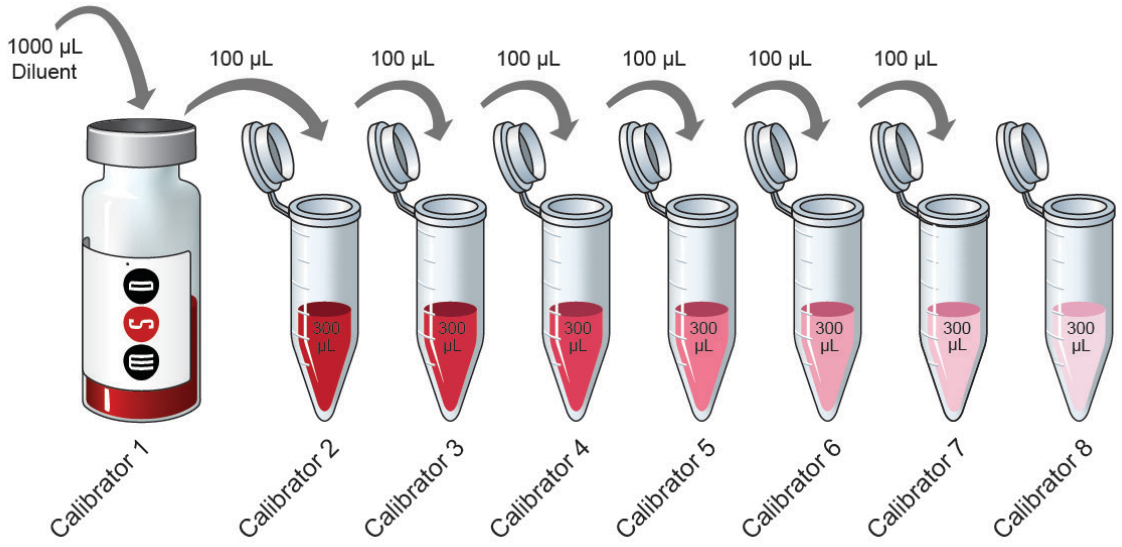

***Figure 3**. Dilution schema for preparation of Calibrator Standards.*

Sample Collection and Handling

Below are general guidelines for mouse sample collection, storage, and handling. If possible, use published guidelines.[92,93] Evaluate sample stability under the selected method as needed.

- Serum and plasma. When preparing serum, allow samples to clot for 2 hours at room temperature, then centrifuge for 20 minutes at 2,000 xg prior to using or freezing. If no particulates are visible, you may not need to centrifuge.
- Other samples. Use immediately or freeze.

Freeze all samples in suitably-sized aliquots; they may be stored at ≤-10 °C until needed. Repeated freezing and thawing of samples is not recommended. After thawing, centrifuge samples at 2,000 xg for 3 minutes to remove particulates prior to sample preparation.

Dilute Samples

Dilute samples with Diluent 41. For mouse serum, plasma, and urine samples, MSD recommends a minimum 4-fold dilution. For example, when running samples in duplicate, add 50 µL of sample to 150 µL of Diluent 41. You may conserve sample volume by using a higher dilution.

Tissue culture supernatants may require additional dilution based on stimulation and analyte concentrations in the sample. Additional diluent can be purchased at www.mesoscale.com.

Prepare Controls

Three levels of multi-analyte lyophilized controls are available for separate purchase from MSD in the TH17 Panel 1 (mouse) Control Pack, catalog # C4246-1. (Controls are included only in V-PLEX Plus kits.)

Reconstitute the lyophilized controls in 250 µL of Diluent 41. After reconstituting, invert at least 3 times (do not vortex). Wait a minimum of 30-45 minutes at room temperature and then vortex briefly using short pulses. Dilute the controls 4-fold in Diluent 41. Add diluted control solutions directly to the MSD TH17 Panel 1 (mouse) plate, and assay as unknown samples.

Reconstituted controls can be stored at 2-8 °C for up 9 days. Controls can also be stored frozen at ≤-70 °C and are stable through 2 freeze-thaws.

For the lot-specific concentration of each analyte in the control pack, refer to the supplied COA. You can also find a copy of the COA at www.mesoscale.com.

Prepare Detection Antibody Solution

MSD provides each detection antibody separately as a 50X stock solution. The working solution is 1X. Prepare the detection antibody solution immediately prior to use.

10-plex TH17 Panel 1 (mouse) kit

For one plate, combine the following detection antibodies and add to 2,400 µL of Diluent 45:

- ❑ 60 µL of SULFO-TAG Anti-ms MIP-3α Antibody
- ❑ 60 µL of SULFO-TAG Anti-ms IL-22 Antibody
- ❑ 60 µL of SULFO-TAG Anti-ms IL-23 Antibody
- ❑ 60 µL of SULFO-TAG Anti-ms IL-17C Antibody
- ❑ 60 µL of SULFO-TAG Anti-ms IL-31 Antibody
- ❑ 60 µL of SULFO-TAG Anti-ms IL-21 Antibody
- ❑ 60 µL of SULFO-TAG Anti-ms IL-17F Antibody
- ❑ 60 µL of SULFO-TAG Anti-ms IL-16 Antibody
- ❑ 60 µL of SULFO-TAG Anti-ms IL-17A Antibody
- ❑ 60 µL of SULFO-TAG Anti-ms IL-17E/IL-25 Antibody

Custom multiplex kits

For 1 plate, combine 60 µL of each supplied detection antibody, then add Diluent 45 to bring the final volume to 3,000 µL.

Individual assay kits

For 1 plate, add 60 µL of the supplied detection antibody to 2,940 µL of Diluent 45.

Prepare Wash Buffer

MSD provides 100 mL of Wash Buffer as a 20X stock solution in the V-PLEX Plus kit. Dilute the stock solution to 1X before use. PBS + 0.05% Tween-20 can be used instead.

For one plate, combine:

- ❑ 15 mL of MSD Wash Buffer (20X)
- ❑ 285 mL of deionized water

Prepare Read Buffer T

MSD provides Read Buffer T as a 4X stock solution. The working solution is 2X.

For one plate, combine:

- ❑ 10 mL of Read Buffer T (4X)
- ❑ 10 mL of deionized water

You may keep excess diluted Read Buffer in a tightly sealed container at room temperature for up to one month.

Prepare MSD Plate

MSD plates are pre-coated with capture antibodies (Figure 1) and exposed to a proprietary stabilizing treatment to ensure the integrity and stability of the immobilized antibodies. Pre-wash plates before use as recommended on the assay protocol.

Protocol

Note: Follow **Reagent Preparation** before beginning this assay protocol.

STEP 1: Wash and Add Sample

- ❑ Wash the plate 3 times with at least 150 µL/well of 1X MSD Wash Buffer.
- ❑ Add 50 µL of prepared samples, calibrators or controls per well. Seal the plate with an adhesive plate seal and incubate at room temperature with shaking for 2 hours.

Note: Washing the plate prior to sample addition is an optional step that may provide greater uniformity of results for certain assays. Analytical parameters, including limits of quantification, recovery of controls, and sample quantification, are not affected by washing the plate prior to sample addition.

STEP 2: Wash and Add Detection Antibody Solution

- ❑ Wash the plate 3 times with at least 150 µL/well of 1X MSD Wash Buffer.
- ❑ Add 25 µL of detection antibody solution to each well. Seal the plate with an adhesive plate seal and incubate at room temperature with shaking for 2 hours.

STEP 3: Wash and Read

- ❑ Wash the plate 3 times with at least 150 µL/well of 1X MSD Wash Buffer.
- ❑ Add 150 µL of 2X Read Buffer T to each well. Analyze the plate on an MSD instrument. Incubation in Read Buffer T is not required before reading the plate.

Alternate Protocols

The suggestions below may be useful as alternate protocols; however, not all were tested using multiple kit lots.

- **Alternate Protocol 1, Extended Sample Incubation:** Incubating samples overnight at 2-8 ºC may improve sensitivity for some assays. See **Appendix A** for specific assays that may benefit from this alternate protocol.
- **Alternate Protocol 2, Reduced Wash:** For tissue culture samples, you may simplify the protocol by eliminating one of the wash steps. After incubating diluted sample, calibrator, or control, add detection antibody solution to the plate without decanting or washing the plate. See **Appendix A** for assay performance using this protocol.
- **Alternate Protocol 3, Dilute-in-Plate:** To limit sample handling, you may dilute samples and controls in the plate. For 4-fold dilution, add 37.5 µL of assay diluent to each sample/control well, and then add 12.5 µL of neat control or sample. Calibrators should not be diluted in the plate; add 50 µL of each calibrator directly into empty wells. Tests conducted according to this alternate protocol produced results that were similar to the recommended protocol (data not shown).

Validation

MSD's V-PLEX products are analytically validated following fit-for-purpose principles[91] and MSD design control procedures. V-PLEX assay components go through an extensive critical reagents program to ensure that the reagents are controlled and well characterized. Prior to the release of each V-PLEX panel, at least three independent kit lots are produced. Using results from multiple runs (typically greater than 50) and multiple operators, these lots are used to establish production specifications for sensitivity, specificity, accuracy, and precision. During validation, each individual assay is analytically validated as a singleplex and is also independently evaluated as a multiplex component by running the full multiplex plate using only the single detection antibody for that assay. These results are compared with the results from the multiplex panel when using all detection antibodies. This demonstrates that each assay is specific and independent, allowing them to be multiplexed in any combination. The COA provided with each kit outlines the kit release specifications for sensitivity, specificity, accuracy, and precision.

- ### Dynamic Range

  Calibration curve concentrations for each assay are optimized for a maximum dynamic range while maintaining enough calibration points near the bottom of the curve to ensure a proper fit for accurate quantification of samples that require high sensitivity.

- ### Sensitivity

  The lower limit of detection (LLOD) is a calculated concentration corresponding to the average signal 2.5 standard deviations above the background (zero calibrator). The LLOD is calculated using results from multiple plates for each lot, and the median and range of calculated LLODs for a representative kit lot are reported in this product insert. The upper limit of quantification (ULOQ) and lower limit of quantification (LLOQ) are established for each lot by measuring multiple levels near the expected LLOQ and ULOQ levels. The final LLOQ and ULOQ specifications for the product are established after assessment of all validation lots.

- ### Accuracy and Precision

  Accuracy and precision are evaluated by measuring calibrators and matrix-based validation samples or controls across multiple runs and multiple lots. For most assays, the results of control measurements fall within 25% of the expected concentration for each run. Precision is reported as the coefficient of variation (CV). Intra-run CVs are typically below 6%, and inter-run CVs are typically below 10%. Rigorous management of inter-lot reagent consistency and calibrator production results in typical inter-lot CVs below 10%. Validation lots are compared using controls and at least 30 samples in various sample matrices. Samples are well correlated with an inter-lot bias typically below 10%.

- ### Matrix Effects and Samples

  Matrix effects from serum, plasma, urine, and cell culture media are measured as part of development and validation. Dilution linearity and spike recovery studies are performed on individual samples to assess variability of results due to matrix effects. The sample dilution suggested in the protocol gives an appropriate dilution factor for all assays in the multiplex. Some assays may benefit from lower or higher dilution factors, depending on the samples and application (data are provided in this product insert). In addition to the matrices listed above, cell lines and splenocytes that have been stimulated to generate elevated levels of analytes are tested. Results confirm measurement of native proteins at concentrations that are sometimes higher than those found in individual native samples.

- **Specificity**

  The specificity of both capture and detection antibodies is measured during assay development. Antibody specificity is assessed by first running each assay using the multiplex plate with assay-specific detection antibody and assay-specific calibrator. These results are compared to the assay's performance when the plate is run 1) with the multi-analyte calibrator and assay-specific detection antibodies, and 2) with assay-specific calibrator and all detection antibodies. For each validation lot and for product release, assay specificity is measured using a multi-analyte calibrator and individual detection antibodies. The calibrator concentration used for specificity testing is chosen to ensure that the specific signal is greater than 50,000 counts.

  In addition to measuring the specificity of antibodies to analytes in the multiplex kit, specificity and interference from other related markers are tested during development. This includes evaluation of selected related proteins and receptors or binding partners.

- **Assay Robustness and Stability**

  The robustness of the assay protocol is assessed by examining the boundaries of the selected incubation times and evaluating the stability of assay components during the experiment and the stability of reconstituted lyophilized components during storage. For example, the stability of reconstituted calibrator is assessed in real time over a 30-day period. Assay component (calibrator, antibody, control) stability was assessed through freeze–thaw testing and accelerated stability studies. The validation program includes a real-time stability study with scheduled performance evaluations of complete kits for up to 54 months from date of manufacture.

Representative data from the validation studies are presented in the following sections. The calibration curve and measured limits of detection for each lot can be found in the lot-specific COA that is included with each kit and available for download at www.mesoscale.com.

Analysis of Results

The calibration curves used to calculate analyte concentrations were established by fitting the signals from the calibrators to a 4-parameter logistic (or sigmoidal dose-response) model with a $1/Y^2$ weighting. The weighting function provides a better fit of data over a wide dynamic range, particularly at the low end of the calibration curve. Analyte concentrations were determined from the ECL signals by back-fitting to the calibration curve. These assays routinely have a wide dynamic range, which allows accurate quantification of samples without the need for multiple dilutions or repeated testing. The calculations to establish calibration curves and determine concentrations were carried out using the MSD DISCOVERY WORKBENCH® analysis software.

Best quantification of unknown samples will be achieved by generating a calibration curve for each plate using a minimum of two replicates at each calibrator level.

Typical Data

Data from the TH17 Panel 1 (mouse) were collected over one month of testing by five operators (20 runs in total). Calibration curve accuracy and precision were assessed for two kit lots. Representative data from one lot are presented below. (Data from individual assays are presented in Appendix B.) The multiplex panel was tested with individual detection antibodies to demonstrate that the assays are independent of one another. Appendix C compares results for each assay in the kit when the panel is run using the individual detection antibody versus all detection antibodies. The calibration curves were comparable. Calibration curves for each lot are presented in the lot-specific COA.

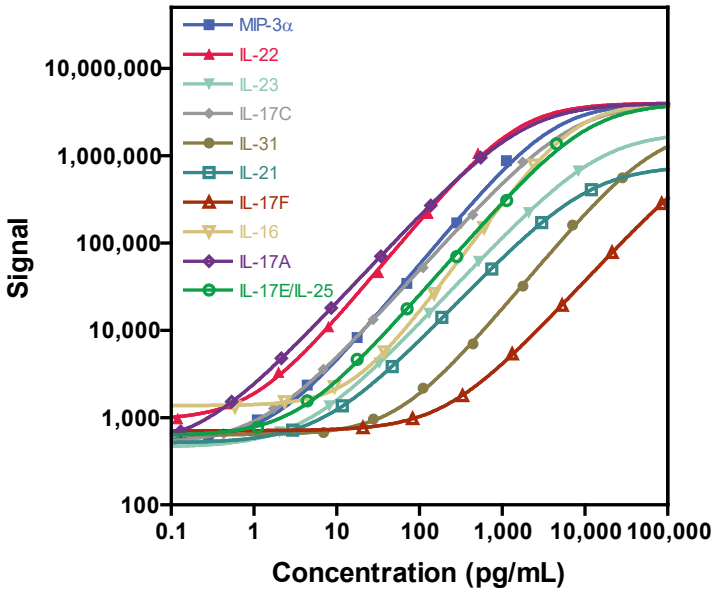

Figure 4. *Typical calibration curves for the TH17 Panel 1 (mouse) assays.*

Sensitivity

The LLOD is a calculated concentration corresponding to the signal 2.5 standard deviations above the background (zero calibrator). The LLOD shown below was calculated based on 60 runs.

The ULOQ is the highest concentration at which the CV of the calculated concentration is <20% and the recovery of each analyte is within 75% to 125% of the known value.

The LLOQ is the lowest concentration at which the CV of the calculated concentration is <20% (<25% for IL-23, IL-21, and IL-16) and the recovery of each analyte is within 75% to 125% of the known value.

The quantitative range of the assay lies between the LLOQ and ULOQ.

The LLOQ and ULOQ are verified for each kit lot and the results are provided in the lot-specific COA that is included with each kit and available at www.mesoscale.com.

Table 5. LLOD, LLOQ, and ULOQ for each analyte in the TH17 Panel 1 (mouse) Kit

	Median LLOD (pg/mL)	LLOD Range (pg/mL)	LLOQ (pg/mL)	ULOQ (pg/mL)
MIP-3α	0.389	0.191-1.01	3.42	530
IL-22	0.136	0.064-0.281	1.58	380
IL-23*	0.899	0.367-2.91	4.19	7,600
IL-17C	0.313	0.117-0.766	0.971	1,200
IL-31	8.57	3.51-17.5	22.6	21,000
IL-21*	1.74	0.820-3.95	12.1	9,300
IL-17F	51.4	17.1-117	320	52,000
IL-16*	4.65	1.15-12.0	15.0	1,800
IL-17A	0.056	0.031-0.144	0.255	360
IL-17E/IL-25	0.630	0.200-2.05	4.54	3,300

*The LLOQ CV is <25% for these assays.

Precision

Controls were made by spiking calibrator into non-mouse serum matrix at three levels within the quantitative range of the assay. Analyte levels were measured by five operators using a minimum of three replicates on 60 runs over 7 days. Results are shown below. While a typical specification for precision is a concentration CV of less than 20% for controls on both intra- and inter-day runs, for this panel, the data shows most assays are below 10%.

Average intra-run %CV is the average %CV of the control replicates within an individual run across 60 runs (four kit lots).

Inter-run %CV is the variability of controls across 15 runs within a single kit lot.

Inter-lot %CV is the variability of controls across 4 kit lots (total of 60 runs).

Table 6. Intra-run and Inter-run %CVs for each analyte in the TH17 Panel 1 (mouse) Kit

	Control	Average Conc. (pg/mL)	Average Intra-run %CV	Average Inter-run %CV	Average Inter-lot %CV
MIP-3α	Control 1	841	5.6	10.3	8.8
	Control 2	211	5.1	11.7	10.1
	Control 3	57.9	6.2	12.7	11.5
IL-22	Control 1	421	2.6	3.8	5.0
	Control 2	129	3.0	6.4	6.3
	Control 3	41.5	4.2	9.2	8.6
IL-23	Control 1	6,928	6.5	15.3	12.0
	Control 2	1,392	5.6	14.1	11.3
	Control 3	270	6.2	14.0	12.5
IL-17C	Control 1	1,514	3.4	5.9	6.0
	Control 2	241	3.9	7.9	8.3
	Control 3	54.3	5.4	10.3	10.4
IL-31	Control 1	23,383	3.8	7.7	6.7
	Control 2	4,798	4.5	8.9	8.2
	Control 3	1,008	4.5	11.5	10.6
IL-21	Control 1	11,716	7.1	11.5	13.6
	Control 2	2,088	7.2	13.3	15.0
	Control 3	279	7.4	12.4	16.7
IL-17F	Control 1	49,138	8.8	12.2	11.6
	Control 2	10,499	9.4	12.0	12.6
	Control 3	2,266	9.5	15.4	15.2
IL-16	Control 1	1,968	7.4	14.9	10.8
	Control 2	1,033	8.2	14.3	11.5
	Control 3	635	8.2	11.8	11.2
IL-17A	Control 1	461	2.5	3.7	4.1
	Control 2	75.5	2.7	5.5	5.8
	Control 3	14.7	3.3	10.5	8.8
IL-17E/IL-25	Control 1	3,484	5.0	11.7	9.3
	Control 2	889	5.2	13.6	10.6
	Control 3	208	6.3	16.1	14.0

Dilution Linearity

To assess linearity, normal mouse serum, EDTA plasma, heparin plasma, citrate plasma, and urine from a commercial source as well as cell culture supernatants were spiked with recombinant calibrators and diluted 4-fold, 8-fold, 16-fold, and 32-fold before testing. Percent recovery at each dilution level was normalized to the dilution-adjusted, 4-fold concentration. The average percent recovery is based on samples within the quantitative range of the assay.

$$\%\ Recovery = \frac{measured\ concentration}{expected\ concentration} * 100$$

Table 7. Analyte percent recovery at various dilutions in serum, EDTA plasma, heparin plasma, citrate plasma, and urine samples

		MIP-3α		IL-22		IL-23		IL-17C		IL-31	
Sample Type	Fold Dilution	Average % Recovery	% Recovery Range	Average % Recovery	% Recovery Range	Average % Recovery	% Recovery Range	Average % Recovery	% Recovery Range	Average % Recovery	% Recovery Range
Serum (N=10)	8	96	90 - 103	113	109 - 118	91	86 - 100	118	113 - 126	118	109 - 130
	16	89	80 - 101	115	105 - 124	99	93 - 105	126	111 - 143	136	123 - 152
	32	92	82 - 107	118	104 - 130	91	84 - 105	126	115 - 146	155	137 - 178
EDTA Plasma (N=10)	8	97	92 - 101	105	99 - 113	98	94 - 107	107	99 - 112	106	93 - 120
	16	99	94 - 104	106	92 - 120	97	88 - 102	104	97 - 109	110	90 - 133
	32	100	95 - 107	102	85 - 120	86	75 - 94	98	92 - 104	109	86 - 135
Cell Culture Media (N=6)	8	97	92 - 108	99	94 - 110	91	83 - 99	98	96 - 103	88	83 - 92
	16	93	82 - 103	94	85 - 103	88	81 - 92	98	90 - 110	81	75 - 86
	32	96	87 - 105	93	80 - 100	78	65 - 88	94	88 - 107	80	71 - 85
Citrate Plasma (N=10)	8	104	94 - 107	107	104 - 112	97	93 - 105	106	104 - 114	114	109 - 126
	16	105	93 - 112	113	108 - 119	101	91 - 109	109	96 - 120	135	125 - 149
	32	106	95 - 115	114	108 - 121	95	83 - 103	111	97 - 126	139	124 - 158
Heparin Plasma (N=10)	8	92	78 - 97	107	104 - 113	106	95 - 116	123	118 - 128	127	116 - 145
	16	95	86 - 98	111	106 - 119	111	95 - 122	134	130 - 138	156	138 - 180
	32	96	86 - 100	116	108 - 123	105	93 - 114	142	138 - 146	171	155 - 202
Urine (N=10)	8	107	99 - 119	100	98 - 103	95	88 - 101	104	101 - 113	95	89 - 104
	16	108	100 - 122	99	96 - 102	92	86 - 101	104	97 - 120	92	84 - 104
	32	117	107 - 132	98	93 - 102	87	79 - 104	103	96 - 118	90	82 - 103

Table 7 continued.

		IL-21		IL-17F		IL-16		IL-17A		IL-17E/IL-25	
Sample Type	Fold Dilution	Average % Recovery	% Recovery Range	Average % Recovery	% Recovery Range	Average % Recovery	% Recovery Range	Average % Recovery	% Recovery Range	Average % Recovery	% Recovery Range
Serum (N=10)	8	102	97 - 108	92	86 - 99	110	104 - 114	112	107 - 117	107	102 - 113
	16	103	94 - 110	92	81 - 103	108	94 - 120	120	108 - 130	109	100 - 122
	32	98	87 - 105	88	76 - 101	104	91 - 114	114	106 - 123	101	90 - 114
EDTA Plasma (N=10)	8	100	96 - 106	92	86 - 96	107	98 - 122	106	99 - 116	123	98 - 135
	16	98	90 - 107	86	75 - 92	106	98 - 122	104	95 - 115	121	95 - 141
	32	93	84 - 102	75	62 - 88	100	92 - 115	97	91 - 102	109	92 - 116
Cell Culture Media (N=6)	8	105	96 - 123	94	89 - 104	101	98 - 109	98	95 - 102	103	98 - 110
	16	97	87 - 115	86	79 - 95	96	90 - 105	95	90 - 99	100	91 - 110
	32	96	88 - 109	82	69 - 97	100	93 - 109	91	79 - 98	102	93 - 112
Citrate Plasma (N=10)	8	105	100 - 112	93	86 - 103	104	102 - 108	105	102 - 110	102	95 - 109
	16	110	101 - 116	92	84 - 97	108	102 - 115	106	104 - 109	105	98 - 112
	32	107	102 - 114	85	76 - 92	108	100 - 116	104	99 - 108	101	92 - 108
Heparin Plasma (N=10)	8	133	119 - 140	102	98 - 107	106	101 - 109	106	102 - 109	103	98 - 109
	16	159	138 - 169	105	92 - 117	109	102 - 115	108	105 - 112	106	100 - 112
	32	153	129 - 166	96	79 - 113	115	108 - 121	106	102 - 113	109	105 - 114
Urine (N=10)	8	102	74 - 114	100	96 - 107	103	99 - 107	101	99 - 103	92	85 - 95
	16	98	71 - 110	98	94 - 102	108	98 - 115	97	95 - 100	89	80 - 95
	32	92	67 - 105	92	84 - 97	103	86 - 118	93	89 - 96	86	79 - 96

Spike Recovery

Spike recovery measurements were evaluated for different sample types throughout the quantitative range of the assays. Multiple pooled mouse samples (serum, EDTA plasma, heparin plasma, citrate plasma, and urine) were obtained from a commercial source. These samples, along with cell culture supernatants, were spiked with calibrators at three levels (high, mid, and low) then diluted 4-fold. The average % recovery for each sample type is reported along with %CV and % recovery range.

$$\%\ Recovery = \frac{measured\ concentration}{expected\ concentration} * 100$$

Table 8. Analyte percent recovery at various dilutions in serum, EDTA plasma, heparin plasma, citrate plasma, and urine samples

	Serum (N=6)			EDTA Plasma (N=6)			Cell Culture Media (N=6)		
	Average % Recovery	%CV	% Recovery Range	Average % Recovery	%CV	% Recovery Range	Average % Recovery	%CV	% Recovery Range
MIP-3α	98	6.2	89-111	80	4.3	73-85	115	7.8	99-132
IL-22	82	4.3	76-90	85	6.7	77-94	114	6.1	99-130
IL-23	88	8.6	68-103	88	6.7	72-97	108	11.2	87-133
IL-17C	70	8.5	54-83	77	5.5	68-85	103	9.6	82-121
IL-31	59	12.2	48-78	79	11.4	61-113	109	10.0	85-130
IL-21	90	13.5	72-123	107	9.1	84-126	103	14.1	75-156
IL-17F	110	15.6	76-140	113	7.8	92-127	113	7.2	97-129
IL-16	NA	NA	NA	103	3.3	101-107	104	12.7	81-134
IL-17A	84	6.8	74-95	84	6.1	75-100	106	7.8	92-121
IL-17E/ IL-25	100	7.4	87-119	81	7.4	71-94	92	9.0	70-110

	Citrate Plasma (N=6)			Heparin Plasma (N=6)			Urine (N=5)		
	Average % Recovery	%CV	% Recovery Range	Average % Recovery	%CV	% Recovery Range	Average % Recovery	%CV	% Recovery Range
MIP-3α	87	6.0	77-94	103	5.4	95-116	93	11.0	75-110
IL-22	86	4.6	78-92	84	3.2	79-88	110	6.3	95-123
IL-23	88	9.4	64-99	85	9.1	61-97	101	14.4	70-126
IL-17C	77	9.5	63-90	71	8.0	61-86	89	14.0	62-110
IL-31	69	11.6	54-86	62	20.3	44-105	95	12.8	74-122
IL-21	92	12.3	74-112	61	7.1	55-71	81	17.6	59-110
IL-17F	116	11.3	78-138	108	13.9	67-134	104	6.1	89-116
IL-16	101	6.8	93-110	NA	NA	NA	120	7.0	106-139
IL-17A	95	5.0	83-103	94	5.5	84-105	106	5.3	94-114
IL-17E/ IL-25	90	11.6	73-109	101	7.4	85-116	123	15.7	93-172

NA = Recovery range not available

Specificity

To assess specificity, each assay antibody set in the panel was tested individually. Nonspecific binding was also evaluated with additional recombinant mouse analytes (IFN-γ, IL-1β, IL-10, IL-12p70, IL-2, IL-4, IL-5, IL-6, KC/GRO, TNF-α, IL-9, MCP-1, IL-33, IL-27p28/IL-30, IL-15, MIP-1α, IP-10, MIP-2). Nonspecific binding was less than 0.5% for all assays in the kit.

$$\%\ Nonspecificity = \frac{nonspecific\ signal}{specific\ signal} * 100$$

Nonspecific binding was observed for the mouse IL-17A/F heterodimer on the IL-17A (2.64% IL-17A detect only, 5.88% blended detect) and IL-17F (7.4% IL-17F detect only, 27.8% blended detect) assays.

Cross-species reactivity of the mouse IL-16 assay with human IL-16, but not human IL-21, has been observed.

Stability

The reconstituted calibrator, reconstituted controls, and diluents were tested for freeze–thaw stability. Results (not shown) demonstrated that reconstituted calibrator, reconstituted controls, assay diluents, and antibody diluents can go through three, two, three and one freeze–thaw cycles, respectively, without significantly affecting the performance of the assay. Reconstituted calibrator and controls must be stored frozen at ≤-70 °C. Partially used MSD plates may be sealed and stored up to 30 days at 2–8 °C in the original foil pouch with desiccant. Results from control measurements changed by ≤30% after partially used plates were stored for 30 days. The validation study includes a real-time stability study with scheduled performance evaluations of complete kits for up to 54 months from date of manufacture.

Tested Samples

Normal Samples

Commercially available normal mouse serum, EDTA plasma, heparin plasma, citrate plasma, and urine samples were diluted 4-fold and tested. Results for each sample set are displayed below. Concentrations are corrected for sample dilution. Median and range are calculated from samples with concentrations at or above the LLOD. Percent detected is the percentage of samples with concentrations at or above the LLOD.

Table 9. Normal mouse samples tested in the TH17 Panel 1 (mouse) Kit

Sample Type	Statistic	MIP-3α	IL-22	IL-23	IL-17C	IL-31	IL-21	IL-17F	IL-16	IL-17A	IL-17E/ IL-25
Serum (N=30)	Median (pg/mL)	104	20.2	ND	ND	ND	ND	ND	1,684	3.45	0.067
	Range (pg/mL)	45.3-164	10.5-29.9	ND-9.20	ND -0.302	ND-0.000	ND-6.31	ND -113	1,365-2,098	2.40-9.83	ND -0.871
	% of Samples Detected	100	100	0	0	0	0	10	100	100	0
EDTA Plasma (N=30)	Median (pg/mL)	103	25.3	0.543	1.65	ND	ND	ND	2,148	3.29	3.29
	Range (pg/mL)	68.7-154	17.2-36.2	ND-5.77	ND -4.61	ND- ND	ND -4.38	ND -72.6	1,296-2,887	1.81-5.11	0.841-5.21
	% of Samples Detected	100	100	0	70	0	0	10	100	100	70
Cell Culture Supernatant (N=9)	Median (pg/mL)	2.86	1.113	3.79	0.504	9.1	5.61	149.0	5,738	212.56	0.817
	Range (pg/mL)	ND-447	ND-194	ND-15.1	ND -7.17	ND-218	ND-2,531	ND –106,630	513-15,029	ND –187,789	ND-161
	% of Samples Detected	56	56	33	78	22	44	44	100	78	33
Citrate (N=30)	Median (pg/mL)	115	19.7	2.75	3.75	6.14	3.97	2.37	1,861	3.22	0.830
	Range (pg/mL)	77.5-144	16.4-48.3	ND -16.0	2.61-7.78	ND-101	ND -17.2	ND -252	1,469 -2,495	2.00-6.01	ND -4.74
	% of Samples Detected	100	100	20	100	10	10	30	100	100	10
Urine (N=10)	Median (pg/mL)	85.3	17.6	7.90	2.45	24.4	7.08	36.1	1,260	3.19	0.377
	Range (pg/mL)	48.0-125	12.9-26.9	2.12-15.1	0.577-5.19	ND-97.2	ND-25.8	ND-465	958-1971	1.54-5.49	ND-5.90
	% of Samples Detected	100	100	0	50	0	0	10	100	100	0
Heparin (N=30)	Median (pg/mL)	ND	ND	3.99	ND	ND	ND	ND	ND	0.001	0.210
	Range (pg/mL)	ND-14.8	ND-0.442	ND-30.7	ND-0.717	ND-ND	ND-35.2	ND-2,025	ND-340	ND-1.09	ND-11.8
	% of Samples Detected	10	0	0	0	0	100	0	20	10	0

ND = Non-detectable
NA = Range not available
% Detected = % of samples with concentrations at or above the LLOD

Stimulated Samples

Mouse model cell lines and mouse splenocytes were incubated at 37°C with various stimulating compounds, including Phorbol 12-myristate 13-acetate (PMA), lipopolysaccharide (LPS), Concanavalin A (ConA), and Pokeweed mitogen (PMW). The dilution-adjusted concentrations (pg/mL) for each stimulation model and its unstimulated control are displayed below.

Figure 5. Effect of cell stimulation on cytokine production as measured in the TH17 Panel 1 (mouse) Kit.

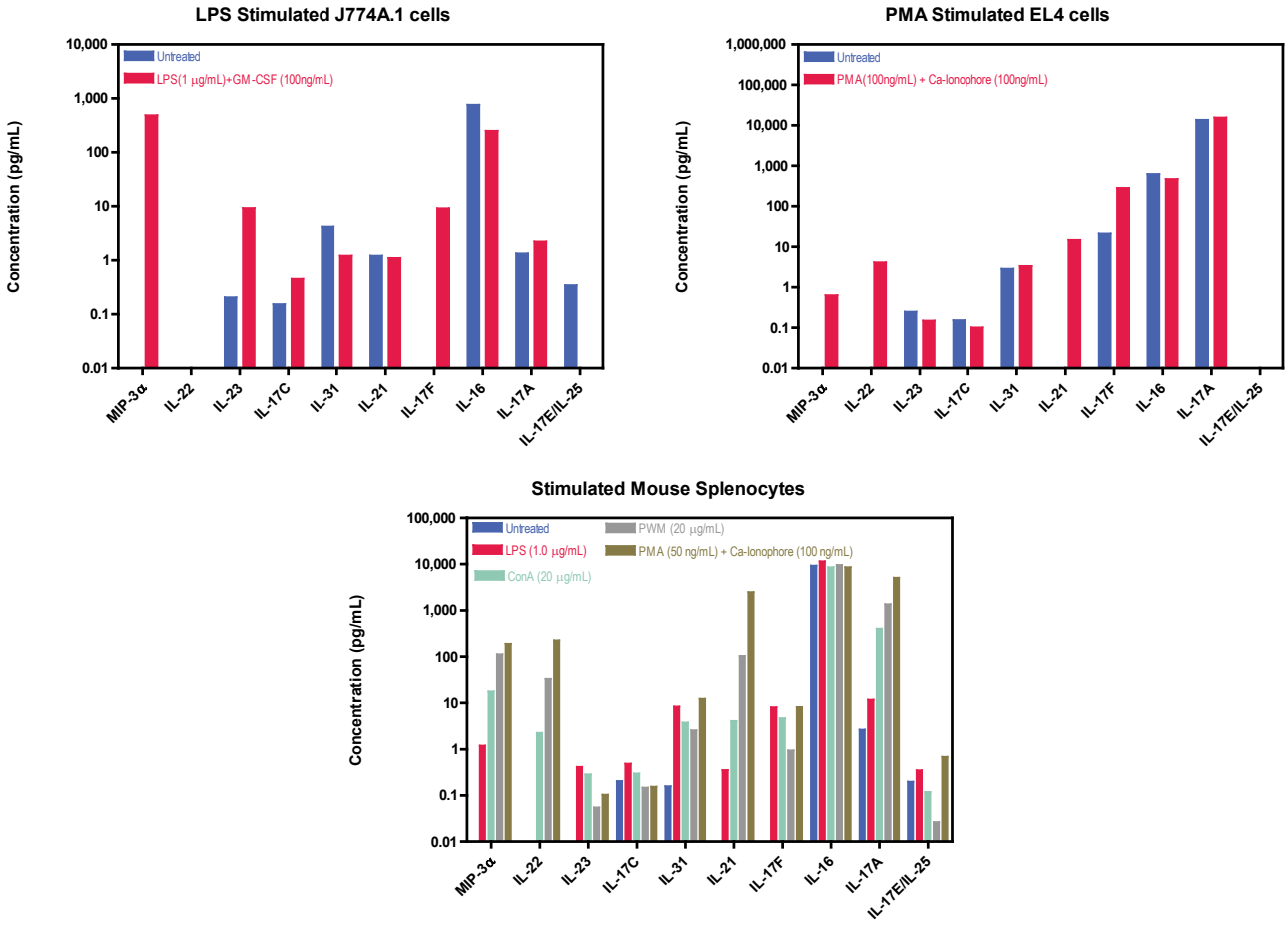

Assay Components

Calibrators

The assay calibrator blend uses the following recombinant mouse proteins:

Table 10. Recombinant mouse proteins used in the Calibrators

Calibrator	Expression System
MIP-3α	*E. coli*
IL-22	*E. coli*
IL-23	Insect cell line
IL-17C	*E. coli*
IL-31	*E. coli*
IL-21	*E. coli*
IL-17F	*E. coli*
IL-16	*E. coli*
IL-17A	*E. coli*
IL-17E/IL-25	*E. coli*

Antibodies

Table 11. Antibody source species

	Source Species		
Analyte	MSD Capture Antibody	MSD Detection Antibody	Assay Generation
MIP-3α	Rat Monoclonal	Goat Polyclonal	A
IL-22	Rat Monoclonal	Goat Polyclonal	A
IL-23	Goat Polyclonal	Rat Monoclonal	A
IL-17C	Rat Monoclonal	Goat Polyclonal	A
IL-31	Goat Polyclonal	Rat Monoclonal	A
IL-21	Goat Polyclonal	Rat Monoclonal	A
IL-17F	Mouse Monoclonal	Rat Monoclonal	A
IL-16	Rat Monoclonal	Goat Polyclonal	A
IL-17A	Rat Monoclonal	Rat Monoclonal	A
IL-17E/IL-25	Rat Monoclonal	Goat Polyclonal	A

References

1. Richmond, J., Tuzova, M., Cruikshank, W. & Center, D. Regulation of cellular processes by interleukin-16 in homeostasis and cancer. *J. Cell. Physiol.* **229,** 139–47 (2014).
2. Zhang, Y. *et al.* Processing and activation of pro-interleukin-16 by caspase-3. *J. Biol. Chem.* **273,** 1144–9 (1998).
3. Chupp, G. L. *et al.* Tissue and T cell distribution of precursor and mature IL-16. *J. Immunol.* **161,** 3114–9 (1998).
4. Seegert, D. *et al.* Increased expression of IL-16 in inflammatory bowel disease. *Gut* **48,** 326–32 (2001).
5. Keane, J. *et al.* Conservation of structure and function between human and murine IL-16. *J. Immunol.* **160,** 5945–54 (1998).
6. Ryan, T. C., Cruikshank, W. W., Kornfeld, H., Collins, T. L. & Center, D. M. The CD4-associated tyrosine kinase p56lck is required for lymphocyte chemoattractant factor-induced T lymphocyte migration. *J. Biol. Chem.* **270,** 17081–6 (1995).
7. Middel, P. *et al.* Interleukin 16 expression and phenotype of interleukin 16 producing cells in Crohn's disease. *Gut* **49,** 795–803 (2001).
8. Pritchard, J., Tsui, S., Horst, N., Cruikshank, W. W. & Smith, T. J. Synovial fibroblasts from patients with rheumatoid arthritis, like fibroblasts from Graves' disease, express high levels of IL-16 when treated with Igs against insulin-like growth factor-1 receptor. *J. Immunol.* **173,** 3564–9 (2004).
9. Ahn, D. S. *et al.* Secretion of IL-16 through TNFR1 and calpain-caspase signaling contributes to MRSA pneumonia. *Mucosal Immunol.* **7,** 1366–74 (2014).
10. Little, F. F. *et al.* Immunomodulatory Effect of Interleukin-16 on Allergic Airway Inflammation. *CHEST J.* **123,** 431S (2003).
11. Zhou, P., Devadas, K., Tewari, D., Jegorow, A. & Notkins, A. L. Processing, secretion, and anti-HIV-1 activity of IL-16 with or without a signal peptide in CD4+ T cells. *J Immunol* **163,** 906–912 (1999).
12. Gu, C., Wu, L. & Li, X. IL-17 family: cytokines, receptors and signaling. *Cytokine* **64,** 477–85 (2013).
13. Iwakura, Y., Ishigame, H., Saijo, S. & Nakae, S. Functional Specialization of Interleukin-17 Family Members. *Immunity* **34,** 149–162 (2011).
14. Gaffen, S. L. Structure and signalling in the IL-17 receptor family. *Nat. Rev. Immunol.* **9,** 556–67 (2009).
15. Chang, S. H. & Dong, C. IL-17F: regulation, signaling and function in inflammation. *Cytokine* **46,** 7–11 (2009).
16. Kastelein, R. A., Hunter, C. A. & Cua, D. J. Discovery and Biology of IL-23 and IL-27: Related but Functionally Distinct Regulators of Inflammation. *Annu. Rev. Immunol.* **25,** 221–242 (2007).
17. Tsai, H.-C., Velichko, S., Hung, L.-Y. & Wu, R. IL-17A and Th17 cells in lung inflammation: an update on the role of Th17 cell differentiation and IL-17R signaling in host defense against infection. *Clin. Dev. Immunol.* **2013,** 267971 (2013).
18. Wakashin, H. *et al.* IL-23 and Th17 cells enhance Th2-cell-mediated eosinophilic airway inflammation in mice. *Am. J. Respir. Crit. Care Med.* **178,** 1023–32 (2008).
19. Ramirez-Carrozzi, V. *et al.* IL-17C regulates the innate immune function of epithelial cells in an autocrine manner. *Nat. Immunol.* **12,** 1159–1166 (2011).
20. Martin, D. A. *et al.* The Emerging Role of IL-17 in the Pathogenesis of Psoriasis: Preclinical and Clinical Findings. *J. Invest. Dermatol.* **133,** 17–26 (2013).
21. Lubberts, E. *et al.* Treatment with a neutralizing anti-murine interleukin-17 antibody after the onset of collagen-induced arthritis reduces joint inflammation, cartilage destruction, and bone erosion. *Arthritis Rheum.* **50,** 650–9 (2004).
22. Patel, D. D., Lee, D. M., Kolbinger, F. & Antoni, C. Effect of IL-17A blockade with secukinumab in autoimmune diseases. *Ann. Rheum. Dis.* **72 Suppl 2,** ii116-23 (2013).
23. Roy, L. Das *et al.* Systemic neutralization of IL-17A significantly reduces breast cancer associated metastasis in arthritic mice by reducing CXCL12/SDF-1 expression in the metastatic niches. *BMC Cancer* **14,** 225 (2014).
24. Fabre, J. *et al.* Targeting the Tumor Microenvironment: The Protumor Effects of IL-17 Related to Cancer Type. *Int. J. Mol. Sci.* **17,** 1433 (2016).
25. Song, X. *et al.* IL-17RE is the functional receptor for IL-17C and mediates mucosal immunity to infection with intestinal pathogens. *Nat. Immunol.* **12,** 1151–1158 (2011).
26. Chang, S. H. *et al.* Interleukin-17C Promotes Th17 Cell Responses and Autoimmune Disease via Interleukin-17 Receptor E. *Immunity* **35,** 611–621 (2011).
27. Pisitkun, P. *et al.* Interleukin-17 Cytokines Are Critical in Development of Fatal Lupus Glomerulonephritis. *Immunity* **37,** 1104–1115 (2012).
28. Jungnickel, C. *et al.* IL-17C mediates the recruitment of tumor-associated neutrophils and lung tumor growth. *Oncogene* **36,** 4182–4190 (2017).
29. Liang, S. C. *et al.* Interleukin (IL)-22 and IL-17 are coexpressed by Th17 cells and cooperatively enhance expression of antimicrobial peptides. *J. Exp. Med.* **203,** 2271–9 (2006).
30. Kawaguchi, M., Kokubu, F., Fujita, J., Huang, S.-K. & Hizawa, N. Role of interleukin-17F in asthma. *Inflamm. Allergy Drug Targets* **8,** 383–9 (2009).
31. Tong, Z. *et al.* A Protective Role by Interleukin-17F in Colon Tumorigenesis. *PLoS One* **7,** e34959 (2012).
32. Dai, Z.-M. Z.-J. *et al.* Role of IL-17A rs2275913 and IL-17F rs763780 polymorphisms in risk of cancer development: an updated meta-analysis. *Sci. Rep.* **6,** 20439 (2016).
33. Jain, M. *et al.* Increased plasma IL-17F levels in rheumatoid arthritis patients are responsive to methotrexate, anti-TNF, and T cell costimulatory modulation. *Inflammation* **38,** 180–6 (2015).
34. Leonard, W. J. & Wan, C.-K. IL-21 Signaling in Immunity. *F1000Research* **5,** 224 (2016).
35. Wei, L., Laurence, A., Elias, K. M. & O'Shea, J. J. IL-21 is produced by Th17 cells and drives IL-17 production in a STAT3-dependent manner. *J. Biol. Chem.* **282,** 34605–10 (2007).
36. Davis, I. D. *et al.* Interleukin-21 signaling: functions in cancer and autoimmunity. *Clin. Cancer Res.* **13,** 6926–32 (2007).
37. Moens, L. & Tangye, S. G. Cytokine-Mediated Regulation of Plasma Cell Generation: IL-21 Takes Center Stage. *Front. Immunol.* **5,** 65 (2014).
38. Parrish-Novak, J. *et al.* Interleukin 21 and its receptor are involved in NK cell expansion and regulation of lymphocyte function. *Nature* **408,** 57–63 (2000).
39. Kasaian, M. T. *et al.* IL-21 limits NK cell responses and promotes antigen-specific T cell activation: a mediator of the transition from innate to adaptive immunity. *Immunity* **16,** 559–69 (2002).
40. Kotlarz, D. *et al.* Loss-of-function mutations in the IL-21 receptor gene cause a primary immunodeficiency syndrome. *J. Exp. Med.* **210,** 433–43 (2013).

41. Wang, G. *et al.* In vivo antitumor activity of interleukin 21 mediated by natural killer cells. *Cancer Res.* **63,** 9016–22 (2003).
42. Zeng, R. *et al.* Synergy of IL-21 and IL-15 in regulating CD8+ T cell expansion and function. *J. Exp. Med.* **201,** 139–48 (2005).
43. Di Fusco, D., Izzo, R., Figliuzzi, M. M., Pallone, F. & Monteleone, G. IL-21 as a therapeutic target in inflammatory disorders. *Expert Opin. Ther. Targets* **18,** 1329–38 (2014).
44. Clarkson, B. D. S. *et al.* T cell–derived interleukin (IL)-21 promotes brain injury following stroke in mice. *J. Exp. Med.* **211,** 595–604 (2014).
45. Meguro, A. *et al.* IL-21 is critical for GVHD in a mouse model. *Bone Marrow Transplant.* **45,** 723–729 (2010).
46. Petrelli, A. *et al.* IL-21 is an antitolerogenic cytokine of the late-phase alloimmune response. *Diabetes* **60,** 3223–34 (2011).
47. Spolski, R. & Leonard, W. J. Interleukin-21: a double-edged sword with therapeutic potential. *Nat. Rev. Drug Discov.* **13,** 379–95 (2014).
48. Dumoutier, L., Louahed, J. & Renauld, J. C. Cloning and characterization of IL-10-related T cell-derived inducible factor (IL-TIF), a novel cytokine structurally related to IL-10 and inducible by IL-9. *J. Immunol.* **164,** 1814–9 (2000).
49. Kreymborg, K. *et al.* IL-22 is expressed by Th17 cells in an IL-23-dependent fashion, but not required for the development of autoimmune encephalomyelitis. *J. Immunol.* **179,** 8098–104 (2007).
50. Weiss, B. *et al.* Cloning of murine IL-22 receptor alpha 2 and comparison with its human counterpart. *Genes Immun.* **5,** 330–336 (2004).
51. Parks, O. B., Pociask, D. A., Hodzic, Z., Kolls, J. K. & Good, M. Interleukin-22 Signaling in the Regulation of Intestinal Health and Disease. *Front. Cell Dev. Biol.* **3,** 85 (2016).
52. Eyerich, S., Eyerich, K., Cavani, A. & Schmidt-Weber, C. IL-17 and IL-22: siblings, not twins. *Trends in Immunology* **31,** 354–361 (2010).
53. Altobelli, E., Angeletti, P. M., Piccolo, D. & De Angelis, R. Synovial Fluid and Serum Concentrations of Inflammatory Markers in Rheumatoid Arthritis, Psoriatic Arthritis and Osteoarthitis: A Systematic Review. *Curr. Rheumatol. Rev.* **13,** 1–1 (2017).
54. Kim, K. W. *et al.* Interleukin-22 promotes osteoclastogenesis in rheumatoid arthritis through induction of RANKL in human synovial fibroblasts. *Arthritis Rheum.* **64,** 1015–1023 (2012).
55. Kong, X., Feng, D., Mathews, S. & Gao, B. Hepatoprotective and anti-fibrotic functions of interleukin-22: Therapeutic potential for the treatment of alcoholic liver disease. *Journal of Gastroenterology and Hepatology (Australia)* **28,** 56–60 (2013).
56. Besnard, A. G. *et al.* Dual role of IL-22 in allergic airway inflammation and its cross-talk with IL-17A. *Am. J. Respir. Crit. Care Med.* **183,** 1153–1163 (2011).
57. Yannam, G. R., Gutti, T. & Poluektova, L. Y. IL-23 in infections, inflammation, autoimmunity and cancer: Possible role in HIV-1 and AIDS. *Journal of Neuroimmune Pharmacology* **7,** 95–112 (2012).
58. Damsker, J. M., Hansen, A. M. & Caspi, R. R. Th1 and Th17 cells: Adversaries and collaborators. *Annals of the New York Academy of Sciences* **1183,** 211–221 (2010).
59. Boniface, K., Blom, B., Liu, Y. J. & De Waal Malefyt, R. From interleukin-23 to T-helper 17 cells: Human T-helper cell differentiation revisited. *Immunological Reviews* **226,** 132–146 (2008).
60. Langrish, C. L. *et al. IL-12 and IL-23: Master regulators of innate and adaptive immunity. Immunological Reviews* **202,** 96–105 (2004).
61. Toussirot, E. The IL23/Th17 Pathway as a Therapeutic Target in Chronic Inflammatory Diseases. *Inflamm. Allergy-Drug Targets* **11,** 159–168 (2012).
62. Zhang, Q., Putheti, P., Zhou, Q., Liu, Q. & Gao, W. *Structures and biological functions of IL-31 and IL-31 receptors. Cytokine and Growth Factor Reviews* **19,** 347–356 (2008).
63. Ferretti, E., Corcione, A. & Pistoia, V. The IL-31/IL-31 receptor axis: general features and role in tumor microenvironment. *J. Leukoc. Biol.* **102,** 711–717 (2017).
64. Cornelissen, C., Lüscher-Firzlaff, J., Baron, J. M. & Lüscher, B. *Signaling by IL-31 and functional consequences. European Journal of Cell Biology* **91,** 552–566 (2012).
65. Nobbe, S. *et al.* IL-31 expression by inflammatory cells is preferentially elevated in atopic dermatitis. *Acta Derm. Venereol.* **92,** 24–8 (2012).
66. Auriemma, M., Vianale, G., Amerio, P. & Reale, M. Cytokines and T cells in atopic dermatitis. *Eur. Cytokine Netw.* **24,** 37–44 (2013).
67. Andoh, A. *et al.* Mucosal cytokine network in inflammatory bowel disease. *World J. Gastroenterol.* **14,** 5154–61 (2008).
68. Ip, W. K. *et al.* Interleukin-31 induces cytokine and chemokine production from human bronchial epithelial cells through activation of mitogen-activated protein kinase signalling pathways: implications for the allergic response. *Immunology* **122,** 532–41 (2007).
69. Ferretti, E. *et al.* The interleukin (IL)-31/IL-31R axis contributes to tumor growth in human follicular lymphoma. *Leukemia* **29,** 958–67 (2015).
70. Schutyser, E., Struyf, S. & Van Damme, J. The CC chemokine CCL20 and its receptor CCR6. *Cytokine Growth Factor Rev.* **14,** 409–26 (2003).
71. Tanaka, Y. *et al.* Selective expression of liver and activation-regulated chemokine (LARC) in intestinal epithelium in mice and humans. *Eur. J. Immunol.* **29,** 633–642 (1999).
72. Pérez-Cañadillas, J. M. *et al.* NMR solution structure of murine CCL20/MIP-3alpha, a chemokine that specifically chemoattracts immature dendritic cells and lymphocytes through its highly specific interaction with the beta-chemokine receptor CCR6. *J. Biol. Chem.* **276,** 28372–9 (2001).
73. Meares, G. P., Ma, X., Qin, H. & Benveniste, E. N. Regulation of CCL20 expression in astrocytes by IL-6 and IL-17. *Glia* **60,** 771–781 (2012).
74. Reboldi, A. *et al.* C-C chemokine receptor 6–regulated entry of TH-17 cells into the CNS through the choroid plexus is required for the initiation of EAE. *Nat. Immunol.* **10,** 514–523 (2009).
75. Ambrosini, E., Columba-Cabezas, S., Serafini, B., Muscella, A. & Aloisi, F. Astrocytes are the major intracerebral source of macrophage inflammatory protein-3??/CCL20 in relapsing experimental autoimmune encephalomyelitis and in vitro. *Glia* **41,** 290–300 (2003).
76. Baba, M. *et al.* Identification of CCR6, the specific receptor for a novel lymphocyte-directed CC chemokine LARC. *J. Biol. Chem.* **272,** 14893–8 (1997).
77. Taub, D. D. *et al.* Chemokines and T lymphocyte activation: I. Beta chemokines costimulate human T lymphocyte activation in vitro. *J. Immunol.* **156,** 2095–2103 (1996).
78. Kondo, T., Takata, H. & Takiguchi, M. Functional expression of chemokine receptor CCR6 on human effector memory CD8+ T cells. *Eur. J. Immunol.* **37,** 54–65 (2007).
79. Nandi, B. *et al.* CCR6, the sole receptor for the chemokine CCL20, promotes spontaneous intestinal tumorigenesis. *PLoS One* **9,** e97566 (2014).
80. Furumoto, K., Soares, L., Engleman, E. G. & Merad, M. Induction of potent antitumor immunity by in situ targeting of intratumoral DCs. *J. Clin. Invest.* **113,** 774–783 (2004).
81. Hirota, K. *et al.* Preferential recruitment of CCR6-expressing Th17 cells to inflamed joints via CCL20 in rheumatoid arthritis and its animal model. *J. Exp. Med.* **204,** 2803–2812 (2007).

82. Harper, E. G. *et al.* Th17 cytokines stimulate CCL20 expression in keratinocytes in vitro and in vivo: implications for psoriasis pathogenesis. *J. Invest. Dermatol.* **129,** 2175–2183 (2009).

83. Yao, L., Herlea-Pana, O., Heuser-Baker, J., Chen, Y. & Barlic-Dicen, J. *Roles of the chemokine system in development of obesity, insulin resistance, and cardiovascular disease. Journal of Immunology Research* **2014,** 1–11 (Hindawi, 2014).

84. Lee, S.-M. M. *et al.* Prevention and treatment of diabetes with resveratrol in a non-obese mouse model of type 1 diabetes. *Diabetologia* **54,** 1136–1146 (2011).

85. McGrory, K., Flaitz, C. M. & Klein, J. R. Chemokine changes during oral wound healing. *Biochem. Biophys. Res. Commun.* **324,** 317–320 (2004).

86. Teramoto, K. *et al.* Increased lymphocyte trafficking to colonic microvessels is dependent on MAdCAM-1 and C-C chemokine mLARC/CCL20 in DSS-induced mice colitis. *Clin. Exp. Immunol.* **139,** 421–428 (2005).

87. Dohlman, T. H. *et al.* The CCR6/CCL20 axis mediates Th17 cell migration to the ocular surface in dry eye disease. *Investig. Ophthalmol. Vis. Sci.* **54,** 4081–4091 (2013).

88. Klein, M. *et al.* Leukocyte attraction by CCL20 and its receptor CCR6 in humans and mice with pneumococcal meningitis. *PLoS One* **9,** e93057 (2014).

89. Wan, W. *et al.* Genetic deletion of chemokine receptor Ccr6 decreases atherogenesis in ApoE-deficient mice. *Circ. Res.* **109,** 374–381 (2011).

90. Kallal, L. E., Schaller, M. A., Lindell, D. M., Lira, S. A. & Lukacs, N. W. CCL20/CCR6 blockade enhances immunity to RSV by impairing recruitment of DC. *Eur. J. Immunol.* **40,** 1042–1052 (2010).

91. Lee, J. W. *et al.* Fit-for-purpose method development and validation for successful biomarker measurement. in *Pharmaceutical Research* **23,** 312–328 (2006).

92. Morton, D. B., Abbot, D., Barclay, R. & Close, B. S. Removal of blood from laboratory mammals and birds. *Lab. Anim.* 1–22 (1993). doi:10.1258/002367794780745209

93. Hem, a, Smith, a J. & Solberg, P. Saphenous vein puncture for blood sampling of the mouse, rat, hamster, gerbil, guinea pig, ferret and mink. *Lab. Anim.* **32,** 364–368 (1998).

94. Kay, A. B., Clark, P., Maurer, M. & Ying, S. Elevations in T-helper-2-initiating cytokines (interleukin-33, interleukin-25 and thymic stromal lymphopoietin) in lesional skin from chronic spontaneous ('idiopathic') urticaria. *Br. J. Dermatol.* **172,** 1294–302 (2015).

95. Emamaullee, J. A. *et al.* Inhibition of Th17 cells regulates autoimmune diabetes in NOD mice. *Diabetes* **58,** 1302–11 (2009).

96. Kleinschek, M. A. *et al.* IL-25 regulates Th17 function in autoimmune inflammation. *J. Exp. Med.* **204,** 161–70 (2007).

97. Petersen, B. C., Budelsky, A. L., Baptist, A. P., Schaller, M. A. & Lukacs, N. W. Interleukin-25 induces type 2 cytokine production in a steroid-resistant interleukin-17RB+ myeloid population that exacerbates asthmatic pathology. *Nat. Med.* **18,** 751–8 (2012).

98. Li, L., Lukacs, N. W., Schaller, M. A., Petersen, B. & Baptist, A. P. IL-17RB(+) granulocytes are associated with airflow obstruction in asthma. *Ann. Allergy. Asthma Immunol.* **117,** 674–679 (2016).

99. Furuta, S. *et al.* IL-25 causes apoptosis of IL-25R-expressing breast cancer cells without toxicity to nonmalignant cells. *Sci. Transl. Med.* **3,** 78ra31 (2011).

100. Mombelli, S. *et al.* IL-17A and its homologs IL-25/IL-17E recruit the c-RAF/S6 kinase pathway and the generation of pro-oncogenic LMW-E in breast cancer cells. *Sci. Rep.* **5,** 11874 (2015).

Appendix A

Calibration curves below illustrate the relative sensitivity for each assay under **Alternate Protocols**: Reference Protocol (2-hour sample incubation/2 wash steps, blue curve), in-well dilution (in-well sample dilution, red curve), O/N incubation (overnight sample incubation at 4 °C with shaking, gray curve), and one wash/tissue culture protocol (tissue culture: single wash, green curve).

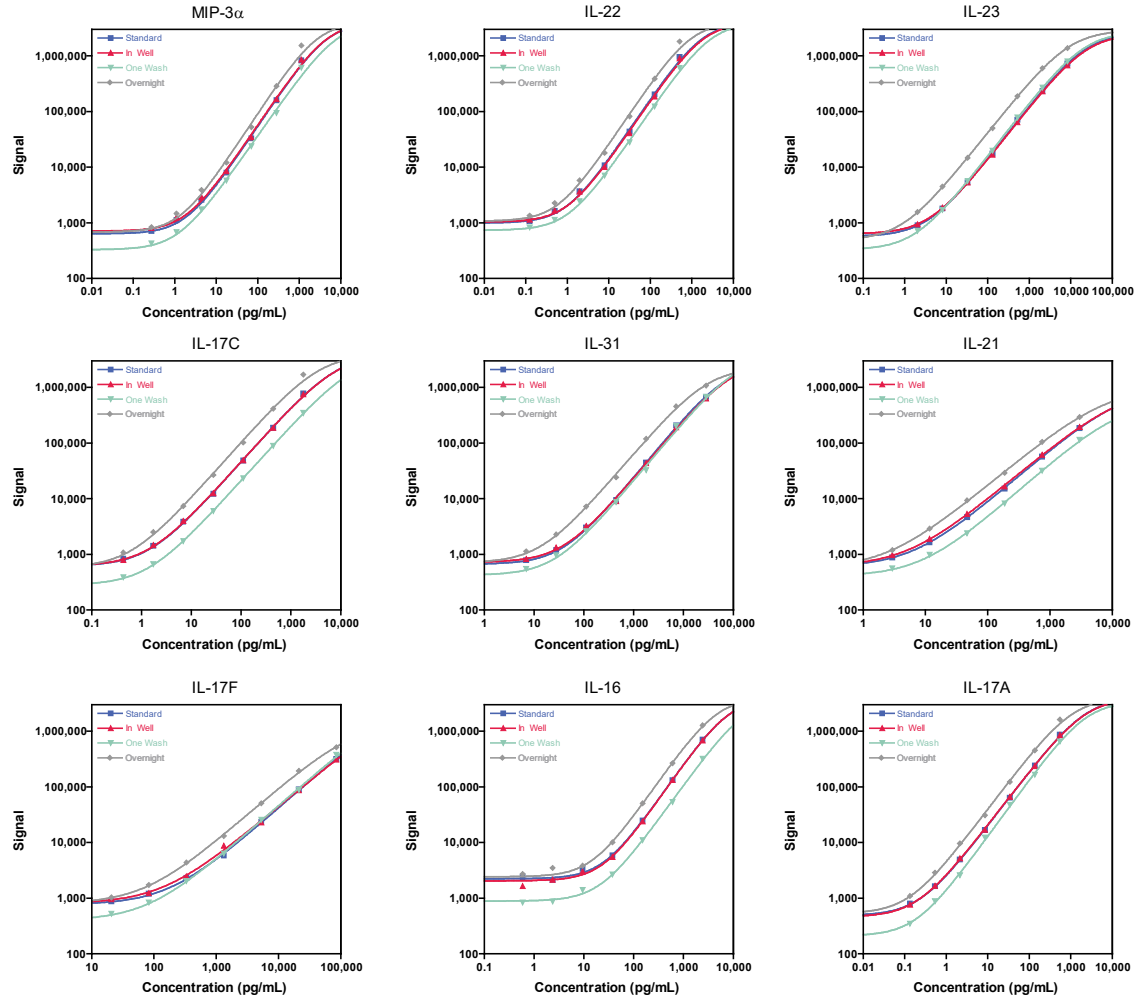

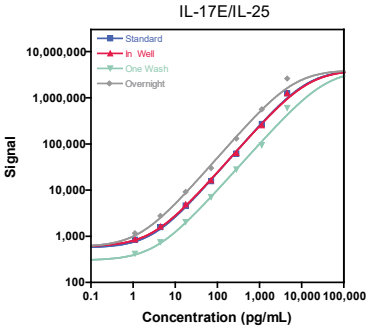

Table 12. Relative sensitivity when using alternate protocols

	LLOD Comparison (pg/mL)			
	Reference Protocol	In-Well Protocol	One Wash Protocol	Overnight Protocol
MIP-3α	0.252	0.227	0.297	0.175
IL-22	0.080	0.194	0.186	0.067
IL-23	0.648	1.53	0.538	0.277
IL-17C	0.681	0.466	0.570	0.070
IL-31	5.14	8.59	4.71	1.62
IL-21	1.44	0.584	1.68	0.296
IL-17F	17.3	37.4	28.7	6.68
IL-16	19.5	28.9	11.9	14.2
IL-17A	0.030	0.029	0.068	0.015
IL-17E/IL-25	0.493	0.343	0.839	0.299

Appendix B

The calibration curves below compare assay performance when the assay is run as an individual assay on a single spot plate (blue curve) vs. on the multiplex plate (red curve).

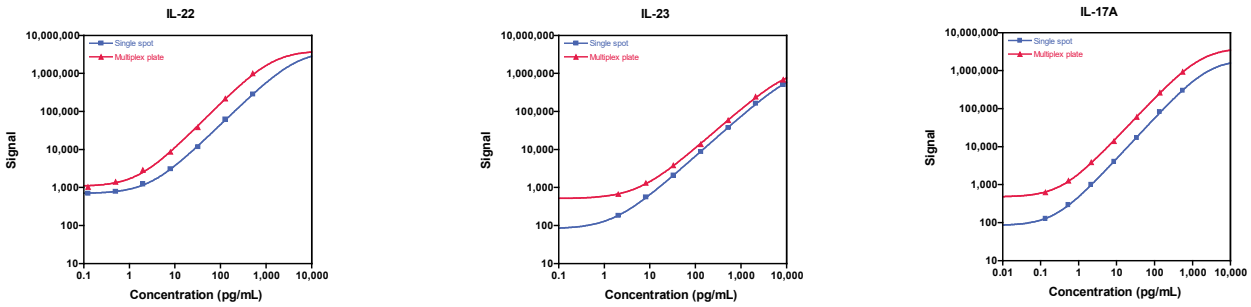

Table 13. Assay performance for individual and 10-plex assays

In general, assays in the single-spot format yielded a lower overall signal compared to the 7-plex format. The spots on single-spot plates have a larger binding surface than those on multiplex plates, but the same amount of calibrator was used for each test; therefore, the bound calibrator was spread over a larger surface area, reducing the average signal.

Note: Assay performance for MIP-3α, IL-17C, IL-31, IL-21, IL-17F, IL-16, and IL-17E/IL-25 are not included since the individual assay is run on a multiplex plate.

	LLOD (pg/mL)	
Assay	Individual	10-plex
IL-22	0.246	0.641
IL-23	1.22	0.542
IL-17A	0.054	0.081

Appendix C

The calibration curves below compare results for each assay in the panel when the assays were run on the 10-spot plate using all 10 detection antibodies (red curve) vs. running each assay using a single, assay-specific detection antibody (blue curve).

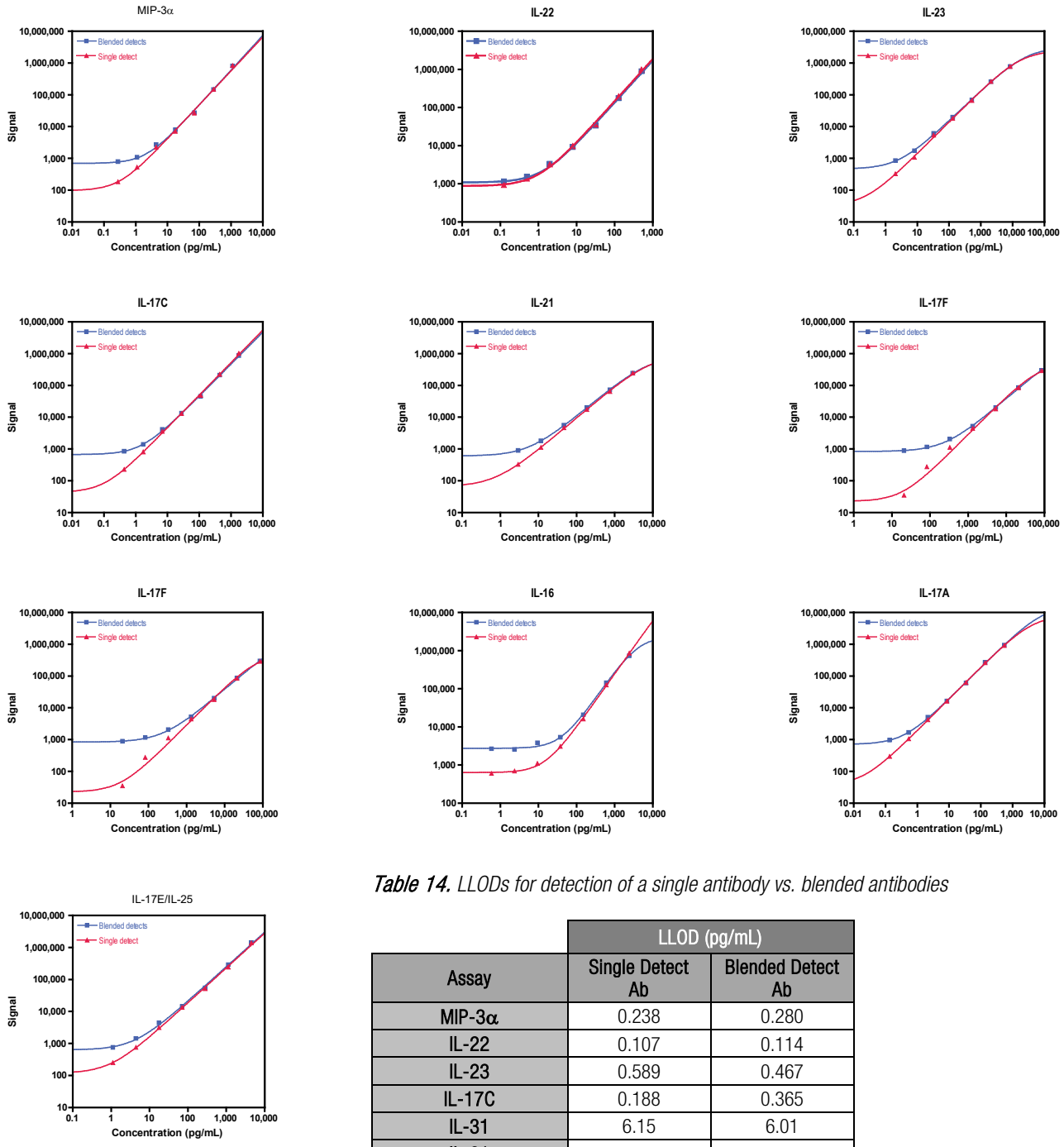

Table 14. LLODs for detection of a single antibody vs. blended antibodies

	LLOD (pg/mL)	
Assay	Single Detect Ab	Blended Detect Ab
MIP-3α	0.238	0.280
IL-22	0.107	0.114
IL-23	0.589	0.467
IL-17C	0.188	0.365
IL-31	6.15	6.01
IL-21	0.847	0.878
IL-17F	49.4	32.7
IL-16	3.15	25.1
IL-17A	0.041	0.058
IL-17E/IL-25	0.539	0.526

Summary Protocol

TH17 Panel 1 (mouse) Kits

MSD provides this summary protocol for your convenience.
Please read the entire detailed protocol prior to performing the TH17 Panel 1 (mouse) assays.

Sample and Reagent Preparation

- ❑ Bring all reagents to room temperature.
- ❑ Prepare calibration solutions in Diluent 41 using the supplied calibrator:
  - Reconstitute the lyophilized calibrator blend.
  - Invert 3 times, equilibrate 30-45 minutes at room temperature.
  - Vortex briefly using short pulses.
  - Perform a series of 4-fold dilution steps and prepare a zero calibrator.
- ❑ Dilute samples and controls 4-fold in Diluent 41 before adding to the plate.
- ❑ Prepare combined detection antibody solution by diluting each 50X detection antibody 50-fold in Diluent 45.
- ❑ Prepare 2X Read Buffer T by diluting 4X Read Buffer T 2-fold with deionized water.

STEP 1: Wash* and Add Sample

- ❑ Wash plate 3 times with at least 150 µL/well of 1X MSD Wash Buffer.
- ❑ Add 50 µL/well of sample (calibrators, controls, or unknowns).
- ❑ Incubate at room temperature with shaking for 2 hours.

STEP 2: Wash and Add Detection Antibody Solution

- ❑ Wash plate 3 times with at least 150 µL/well of 1X MSD Wash Buffer.
- ❑ Add 25 µL/well of 1X detection antibody solution.
- ❑ Incubate at room temperature with shaking for 2 hours.

STEP 3: Wash and Read Plate

- ❑ Wash plate 3 times with at least 150 µL/well of 1X MSD Wash Buffer.
- ❑ Add 150 µL/well of 2X Read Buffer T.
- ❑ Analyze plate on the MSD instrument.

*Note: Washing the plate prior to sample addition is an optional step that may provide greater uniformity of results for certain assays. Analytical parameters including limits of quantification, recovery of controls, and sample quantification, are not affected by washing the plate prior to sample addition.

Catalog Numbers

Kit Name	V-PLEX			V-PLEX Plus*		
	1-Plate Kit	5-Plate kit	25-Plate Kit	1-Plate Kit	5-Plate Kit	25-Plate Kit
Multiplex Kits						
TH17 Panel 1 (mouse)	K15246D-1	K15246D-2	K15246D-4	K15246G-1	K15246G-2	K15246G-4
Individual Assay Kits						
Mouse MIP-3α	K152XDD-1	K152XDD-2	K152XDD-4	K152XDG-1	K152XDG-2	K152XDG-4
Mouse IL-22	K152WVD-1	K152WVD-2	K152WVD-4	K152WVG-1	K152WVG-2	K152WVG-4
Mouse IL-23	K152WWD-1	K152WWD-2	K152WWD-4	K152WWG-1	K152WWG-2	K152WWG-4
Mouse IL-17C	K152WPD-1	K152WPD-2	K152WPD-4	K152WPG-1	K152WPG-2	K152WPG-4
Mouse IL-31	K152XAD-1	K152XAD-2	K152XAD-4	K152XAG-1	K152XAG-2	K152XAG-4
Mouse IL-21	K152WUD-1	K152WUD-2	K152WUD-4	K152WUG-1	K152WUG-2	K152WUG-4
Mouse IL-17F	K152WSD-1	K152WSD-2	K152WSD-4	K152WSG-1	K152WSG-2	K152WSG-4
Mouse IL-16	K152RED-1	K152RED-2	K152RED-4	K152REG-1	K152REG-2	K152REG-4
Mouse IL-17A	K152RFD-1	K152RFD-2	K152RFD-4	K152RFG-1	K152RFG-2	K152RFG-4
Mouse IL-17E/IL-25	K152WRD-1	K152WRD-2	K152WRD-4	K152WRG-1	K152WRG-2	K152WRG-4

*V-PLEX Plus kits include controls, plate seals, and wash buffer. See **Kit Components** for details.

Plate Diagram